

# Sequestosome 1 (p62) mitigates hypoxia-induced cardiac dysfunction by stabilizing hypoxia-inducible factor 1 $\alpha$ and nuclear factor erythroid 2-related factor 2

Rajeshwary Ghosh <sup>1,2\*</sup>, Amir Nima Fatahian<sup>1</sup>, Omid M.T. Rouzbehani<sup>1</sup>, Marissa A. Hathaway<sup>1</sup>, Tariq Mosleh<sup>1</sup>, Vishaka Vinod<sup>1</sup>, Sidney Vowles<sup>1</sup>, Sophie L. Stephens<sup>1</sup>, Siu-Lai Desmond Chung<sup>1</sup>, Isaac D. Cao<sup>1</sup>, Anila Jonnavithula<sup>1</sup>, J. David Symons<sup>1,2</sup>, and Sihem Boudina <sup>1,2\*</sup>

<sup>1</sup>Department of Nutrition and Integrative Physiology, College of Health, University of Utah, Salt Lake City, UT 84112, USA; and <sup>2</sup>Molecular Medicine Program (U2M2), University of Utah, Salt Lake City, UT 84112, USA

Received 1 February 2023; revised 11 September 2023; accepted 3 November 2023; online publish-ahead-of-print 9 February 2024

Time of primary review: 34 days

## Aims

Heart failure due to ischaemic heart disease (IHD) is a leading cause of mortality worldwide. A major contributing factor to IHD-induced cardiac damage is hypoxia. Sequestosome 1 (p62) is a multi-functional adaptor protein with pleiotropic roles in autophagy, proteostasis, inflammation, and cancer. Despite abundant expression in cardiomyocytes, the role of p62 in cardiac physiology is not well understood. We hypothesized that cardiomyocyte-specific p62 deletion evokes hypoxia-induced cardiac pathology by impairing hypoxia-inducible factor 1 $\alpha$  (Hif-1 $\alpha$ ) and nuclear factor erythroid 2-related factor 2 (Nrf2) signalling.

## Methods and results

Adult mice with germline deletion of cardiomyocyte p62 exhibited mild cardiac dysfunction under normoxic conditions. Transcriptomic analyses revealed a selective impairment in Nrf2 target genes in the hearts from these mice. Demonstrating the functional importance of this adaptor protein, adult mice with inducible depletion of cardiomyocyte p62 displayed hypoxia-induced contractile dysfunction, oxidative stress, and cell death. Mechanistically, p62-depleted hearts exhibit impaired Hif-1 $\alpha$  and Nrf2 transcriptional activity. Because findings from these two murine models suggested a cardioprotective role for p62, mechanisms were evaluated using H9c2 cardiomyoblasts. Loss of p62 in H9c2 cells exposed to hypoxia reduced Hif-1 $\alpha$  and Nrf2 protein levels. Further, the lack of p62 decreased Nrf2 protein expression, nuclear translocation, and transcriptional activity. Repressed Nrf2 activity associated with heightened Nrf2-Keap1 co-localization in p62-deficient cells, which was concurrent with increased Nrf2 ubiquitination facilitated by the E3 ligase Cullin 3, followed by proteasomal-mediated degradation. Substantiating our results, a gain of p62 in H9c2 cells stabilized Nrf2 and increased the transcriptional activity of Nrf2 downstream targets.

## Conclusion

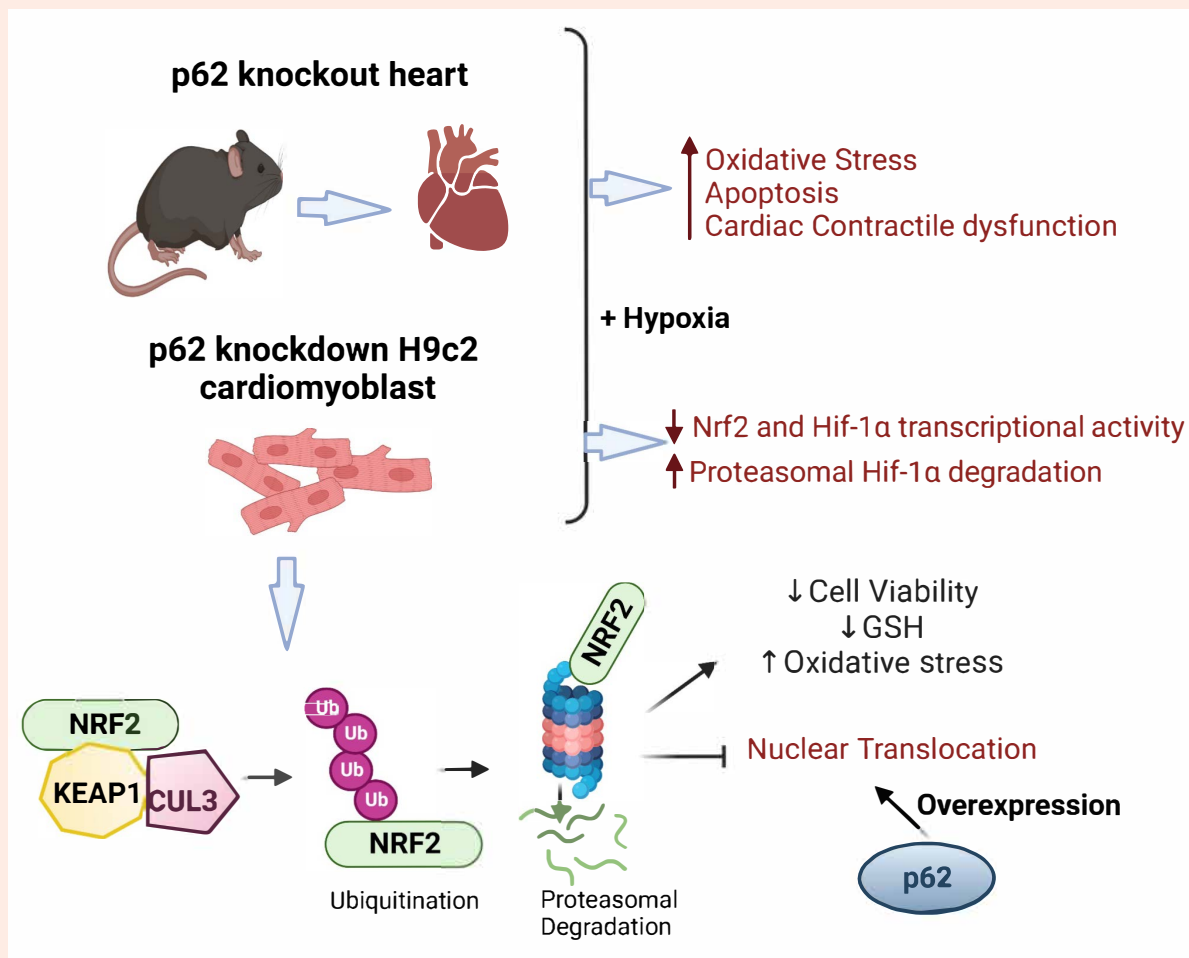
Cardiac p62 mitigates hypoxia-induced cardiac dysfunction by stabilizing Hif-1 $\alpha$  and Nrf2.

\* Corresponding author. Tel: +801 585 0727; fax: +801 585 0701, E-mail: [rghosh7@uthsc.edu](mailto:rghosh7@uthsc.edu) (R.G.); Tel: +801 585 6833; fax +801 585 0701, E-mail: [sboudina@u2m2.utah.edu](mailto:sboudina@u2m2.utah.edu) (S.B.)

© The Author(s) 2024. Published by Oxford University Press on behalf of the European Society of Cardiology.

This is an Open Access article distributed under the terms of the Creative Commons Attribution-NonCommercial License (<https://creativecommons.org/licenses/by-nc/4.0/>), which permits non-commercial re-use, distribution, and reproduction in any medium, provided the original work is properly cited. For commercial re-use, please contact [journals.permissions@oup.com](mailto:journals.permissions@oup.com)

## Graphical Abstract



## Keywords

Oxidative stress • Cardiac function • Nrf2 • Keap1 • Hif1α • Proteasome

## 1. Introduction

Ischaemic heart disease (IHD) is a major cause of mortality in the USA, with over 8.6 million years of life lost and 550 000 deaths reported in 2019.<sup>1</sup> Myocardial ischaemia is a process that occurs when the demand for oxygen ( $O_2$ ) is not met by adequate delivery of blood flow. This can result from occlusion of blood flow either due to the constriction of a coronary artery, thickening of the arterial wall, or formation of a thrombus. In response to  $O_2$  supply: demand mismatching, cardiomyocytes suffer injury or death due to the onset of hypoxia (low  $O_2$ ), a common feature of IHD.

Several multi-factorial pathophysiological processes, including atherosclerosis, inflammation, microvascular coronary dysfunction, endothelial dysfunction, thrombosis, and angiogenesis, contribute to IHD.<sup>2</sup> Further, systemic hypoxia activates the sympathetic limb of the autonomic nervous system, increasing heart rate, pulmonary vascular constriction, reduced arterial  $O_2$ , and systemic vascular resistance, further elevating myocardial  $O_2$  demand.<sup>3,4</sup> As a consequence, the hypoxic heart displays significant cardiac dysfunction, myocyte loss, and redox imbalance.<sup>5</sup> The factors regulating cardiac redox homeostasis during hypoxic stress are not well characterized. Revealing the mechanisms responsible for IHD-mediated redox imbalance is of great importance for the development of new therapies to treat this prevalent condition.

The coordinated response to hypoxia involves activation and stabilization of the transcription factor hypoxia-inducible factor 1α (Hif-1α), resulting in the expression of numerous genes that attempt to balance  $O_2$  delivery and  $O_2$  utilization. Another key response to hypoxia is activation of the nuclear factor erythroid 2-related factor 2 (Nrf2) and Kelch-like ECH-associated protein 1 (Keap1) pathway.<sup>6,7</sup> When intra-cellular redox imbalance exists, Nrf2 binding to Keap1 is disrupted, translocation of unbound Nrf2 to the nucleus is enabled, and binding of Nrf2 to the promoter region of the antioxidant response element is facilitated, resulting in the up-regulation of numerous cytoprotective genes.<sup>8,9</sup>

The multi-functional adaptor protein sequestosome 1 (SQSTM1) (p62) interacts with, and participates in the regulation of, various cell signalling pathways including protein and redox homeostasis.<sup>10</sup> Evidence exists that p62 binds to Keap1 via its Keap1-interacting region (KIR), disrupts Nrf2-Keap1 binding, and allows nuclear translocation of unbound Nrf2 to initiate an antioxidant defence in non-cardiac cells.<sup>11–13</sup> Additionally, p62 positively regulates Hif-1α transcriptional activity and expression of Hif-1α target genes in human adenocarcinoma cells.<sup>14</sup> Emerging evidence suggests that p62 is important in the heart.<sup>15,16</sup> For instance, diastolic dysfunction evoked by ubiquitin proteasome system (UPS) inhibition was more severe in mice with whole-body p62 depletion compared with wild-type (WT) littermates. Further, cardiac p62 is up-regulated in mice with

proteotoxic stress resulting from the expression of the mutant protein crystallin AB (CryAB<sup>R120G</sup>).<sup>17,18</sup> Mechanistically, the authors reported that p62 is required for aggresome-mediated recruitment of soluble misfolded and damaged proteins for degradation. Findings from cultured cardiomyocytes revealed that p62 exerts a feed-forward effect on transcription factor EB, a master regulator of lysosomal biogenesis, upon proteasome inhibition.<sup>18</sup> While these studies indicate that intact p62 has an important role in maintaining cardiac function in the context of proteotoxic stress, the role of p62 in cardiac responses to hypoxia has not been demonstrated. Furthermore, previous studies have employed whole-body knockout of p62, a model that develops obesity and insulin resistance that can indirectly impair cardiac function.<sup>19</sup> To directly assess the role of p62 in the heart in the absence of systemic alterations, we generated mice with conditional deletion of p62 in the heart. Here, we show that (i) under normoxic conditions, mild cardiac dysfunction develops in adult mice with germline depletion of cardiomyocyte p62; (ii) hypoxia causes systolic dysfunction, oxidative stress, and cell death in adult mice with inducible disruption of cardiomyocyte p62; and (iii) hearts from mice with inducible depletion of cardiomyocyte p62 exhibit reduced mRNA expression of Hif-1 $\alpha$  and Nrf2 target genes upon exposure to hypoxia. Considering these findings, mechanisms, whereby p62 regulates Hif-1 $\alpha$  and Nrf2 signalling, were evaluated in H9c2 rat cardiomyoblasts. Of note, we demonstrate that p62 is necessary to stabilize both Hif-1 $\alpha$  and Nrf2 in cardiomyocytes exposed to hypoxia.

## 2. Methods

### 2.1 Generation of mice with germline cardiomyocyte-specific p62 deletion

Animal studies were approved by the University of Utah Institutional Animal Care and Use Committee. All procedures were carried out according to the NIH Guide for the Care and Use of Laboratory Animals. *Sqstm1*<sup>flox/flox</sup> mice, provided by Dr Toru Yanagawa at the University of Tsukuba, were generated by inserting *loxP* sites in the 5' upstream sequence of exon 1 and intron 1 to target the *Sqstm1* locus as previously described.<sup>20</sup> *Sqstm1*<sup>flox/flox</sup> mice were crossed with alpha-myosin heavy chain ( $\alpha$ -MHC)-Cre transgenic mice (B6.FVB-Tg(Myh6-cre)2182Mds/J; Stock No: 011038; Jackson Laboratory) to obtain mice with germline cardiomyocyte-specific p62 deletion (referred to as p62cKO mice). Two-month-old p62cKO and WT mice were utilized to assess cardiac function and to determine Nrf2 nuclear translocation and its target gene expression in the heart. The WT mice were age-, sex-, and background-matched control littermates from the same cohort of p62cKO mice.

### 2.2 Generation of mice with inducible cardiomyocyte-specific p62 depletion

*Sqstm1*<sup>flox/flox</sup> mice were crossed with  $\alpha$ -MHC-Cre-ERT2 (MerCreMer) transgenic mice to direct the expression of a tamoxifen-inducible Cre recombinase. At 2 months of age, inducible cardiomyocyte-specific p62 knockout mice (referred to as p62icKO) were injected intra-peritoneally with 10 mg/mL tamoxifen [prepared in ethanol and sunflower seed oil from *Helianthus annuus* (Sigma)] for 5 consecutive days to induce cardiac p62 deletion. WT littermates (Flox non-Cre and non-flox Cre mice) were treated with the same dose of tamoxifen. The WT mice were control littermates (i.e. age, sex, and background matched) from the same cohort of p62icKO mice. Both p62cKO and p62icKO mice were born at the expected Mendelian frequency and were viable, fertile, and robust.

### 2.3 Echocardiography

Cardiac function and chamber dimensions were measured using transthoracic echocardiography as previously described.<sup>21,22</sup> Two-dimensional guided M-mode and B-mode echocardiography was performed using an echocardiography unit equipped with a 22–55 MHz transducer (Vevo 2100 High Resolution Imaging System, VisualSonics, Toronto, ON,

Canada). Briefly, mice were anesthetized using an inhaled mixture of 1–3% isoflurane and 100% O<sub>2</sub>. Mice were then placed in the supine position on a pre-warmed platform after which chest and abdominal hair was removed using depilatory cream. Ultrasonic gel was applied to the area of interest to enhance the image quality. Heart rate and rectal temperature were continually monitored. A total of four to six long-axis images/mouse were taken and averaged. M-mode images were used to assess ejection fraction (EF) and fractional shortening (FS) via the Vevo LAB 5.6.0 software. Six to eight cardiac cycles per image were obtained by an experimentalist who was blinded to the mouse genotype.

### 2.4 Whole-body hypoxia

After 4 weeks of tamoxifen injection, male and female p62cKO and WT mice were placed in a modular chamber wherein the ambient gas mixture was altered to create a hypoxic environment (i.e. 7% O<sub>2</sub> and 93% N<sub>2</sub>; i.e. hypoxia) for 6 h (10 am to 4 pm). The O<sub>2</sub> percentage within the chamber was monitored throughout and maintained appropriately (BVV Technologies, BWC2-X, Alameda, CA, USA). Animals were provided with food and water ad libitum. Another cohort of mice remained in a cage adjacent to the modular chamber and inhaled room air (i.e. normoxia). After 6-h hypoxia or normoxia, echocardiography was completed as previously described.<sup>21,23</sup> Following echocardiography, mice were immediately euthanized via cervical dislocation and the hearts were collected.

Because echocardiography was completed while mice inhaled 1–3% isoflurane + 100% O<sub>2</sub> for 8 min, concern could be raised that the hypoxia phenotype might be diminished. To address this concern, in preliminary studies, hearts were collected from a subgroup of male and female mice immediately following 6-h hypoxia; i.e. no echocardiography was performed. Results were compared with age-matched male and female mice following 6-h hypoxia + 8-min exposure to 1–3% isoflurane + 100% O<sub>2</sub>, i.e. the time required for echocardiographic analyses. Results shown in [Supplementary material online, Figures S3A and S2A and B](#) indicate Hif-1 $\alpha$  target gene expression was similar between groups.

### 2.5 siRNA transfection

siRNA targeting exon 3 of p62 was used to knockdown p62. Transfection of H9c2 cells was performed as detailed in the [Supplementary material online, Methods](#).<sup>24–26</sup>

### 2.6 Oxyblot assay

An oxyblot assay was performed to detect carbonyl groups introduced into proteins due to oxidative stress in p62cKO or p62icKO hearts vs. their littermate controls and p62 vs. control knockdown cells as described and detailed in the [Supplementary material online, Methods](#).<sup>27,28</sup>

### 2.7 Real-time qPCR

To determine the effect of p62 suppression on the expression of Hif-1 $\alpha$  and Nrf2 target genes in hearts and cells, real-time quantitative polymerase chain reaction (qPCR) analysis was performed as described in the [Supplementary material online, Methods](#).<sup>22,29</sup>

### 2.8 BZ treatment

Cells were treated with bortezomib (BZ) as described and detailed in the [Supplementary material online, Methods](#).<sup>30</sup>

### 2.9 Pull-down of ubiquitinated proteins using TUBES

A tandem ubiquitin-binding entities (TUBES) assay was performed to identify Nrf2 ubiquitination in the presence and absence of p62 as described in the [Supplementary material online, Methods](#).<sup>31,32</sup>

## 2.10 P62 plasmid transfection

For overexpressing p62 in H9c2 cells, a rat p62 gene was cloned in a pshuttle vector under the control of the CMV promoter. The purified plasmid DNA was transfected in H9c2 cells using Lipofectamine 3000 Transfection Reagent (Thermo Fisher Scientific, Cat. No. L3000001),<sup>25</sup> and cells were collected 72 h later.<sup>25</sup>

## 2.11 Statistical analyses

Data are presented as mean  $\pm$  standard deviation of the mean.<sup>33</sup> All statistical analyses were performed using GraphPad Prism software version 9. A *P* value of  $<0.05$  was considered statistically significant. Differences between the two groups were evaluated using an unpaired two-tailed *t*-test. A one-way Analysis of Variance (ANOVA) was used to determine differences among three groups or more. If a significant *P* value was obtained, Sidak's multiple comparisons *post hoc* test was used to identify the location of the differences. A two-way ANOVA was used to determine differences among means with two independent variables. If a significant *P* value was obtained, a Tukey's *post hoc* test was used to identify the location of the differences. Each figure legend contains details concerning the respective statistical test.<sup>33</sup>

Additional procedures concerning genotyping, animal housing, p62cKO and p62icKO mice, RNA sequencing (RNAseq), terminal deoxynucleotidyl transferase dUTP nick end labelling (TUNEL) staining, insulin and glucose tolerance tests, H9c2 cell hypoxia, cell fractionation, the autophagic flux assay, immunoblotting, immunocytochemistry, cycloheximide chase assay, cell viability assays, dichlorodihydrofluorescein diacetate assay, and the glutathione assay are provided in the [Supplementary material online, Methods](#).

## 3. Results

### 3.1 Hearts from germline p62cKO mice display mild systolic dysfunction and attenuated Nrf2 signalling

To study the function of p62 in the absence of metabolic disruptions reported to exist in mice with whole-body p62 deletion,<sup>19</sup> we generated mice with germline cardiomyocyte-specific p62 depletion (p62cKO mice). Knockout of p62 was verified in whole heart lysates obtained from 2-month-old male p62cKO vs. WT mice (see [Supplementary material online, Figure S1A and B](#)).

At 2 months, male p62cKO mice display mild ( $P < 0.05$ ) cardiac dysfunction, including an 18% decrease in EF and a 21% decrease in FS (see [Supplementary material online, Figure S1C and D](#)). As p62 is involved in several signalling pathways (e.g. autophagy, mitophagy, proteasome, cell survival, and inflammation),<sup>34</sup> we used unbiased RNAseq to determine transcriptional changes in the hearts from male p62cKO and WT mice. Results shown in [Supplementary material online, Figure S1E](#) indicate that together with *Sqstm1*, several transcripts of Nrf2 targets (*Gsta2*, *Gsta1*, and *Srxn1*) were reduced in p62cKO vs. WT mice.

The subtle transcriptional alterations observed in response to cardiac p62 deletion were not surprising to us because p62 is as an adaptor protein rather than a transcriptional regulator.<sup>35</sup> Nonetheless, to further define signalling pathways that are altered by the lack of cardiomyocyte p62, we performed a Gene Set Enrichment Analysis. Results indicate the most down-regulated pathway in the p62cKO vs. WT mice involves reactive O<sub>2</sub> species (see [Supplementary material online, Figure S1F](#)), which corroborated our RNAseq findings. We then confirmed the down-regulation of *Sqstm1* and Nrf2 target genes including *Gsta1*, *Gsta2*, and *Nqo1* in the same hearts using qPCR (see [Supplementary material online, Figure S1G](#)). Collectively, these data indicate that Nrf2-mediated transcriptional activity is attenuated in male mice with germline cardiomyocyte-specific p62 depletion.

Our finding that cardiac dysfunction was mild in mice with germline p62 deletion prompted us to investigate whether compensatory mechanisms

were present. Neighbour of BRCA1 gene 1 (Nbr1) is an autophagic adaptor protein that contains p62-like domain architecture, e.g. the Phox and Bem1 domain (PB1), ubiquitin-binding domain (UBA), and the LC3-interacting region domain.<sup>36</sup> The presence of these domains enables Nbr1 to promote autophagic degradation of ubiquitinated targets in a manner that is similar to p62.<sup>37</sup> Strikingly, both Nbr1 mRNA (1.5-fold) and protein (20-fold) expression were higher in hearts from male p62cKO vs. WT mice at 2 months (see [Supplementary material online, Figure S1H–J](#)). The increase in Nbr1 in p62cKO hearts is consistent with a previous study demonstrating that Nbr1 levels increase upon p62 deletion in the brain.<sup>38</sup>

### 3.2 Mice with tamoxifen-inducible cardiomyocyte deletion of p62 display cardiac dysfunction, oxidative stress, and cell death in response to hypoxia

Because a functional redundancy between Nbr1 and p62 might have masked severe cardiac dysfunction which we hypothesized would occur in p62cKO mice, we generated mice with tamoxifen-inducible p62 deletion in cardiomyocytes (aka p62icKO mice; [Supplementary material online, Figure S2A](#)). Deletion of cardiac p62 was validated in 2-month-old female and male mice (see [Supplementary material online, Figure S2B–E](#)). Importantly, no differences existed between p62icKO mice and WT littermates concerning systemic glucose or insulin homeostasis (see [Supplementary material online, Figure S2F–I](#)). Two weeks following tamoxifen injections, under normoxic conditions, we observed that EF and FS were similar between 2-month-old female p62icKO and WT mice ([Figure 1A and C](#) and [Supplementary material online, Figure S2J](#)), whereas both indexes of systolic function were depressed in male p62icKO vs. WT animals ([Figure 1B and C](#) and [Supplementary material online, Figure S2K](#)). To determine whether alpha-MHC-MerCreMer might cause a transient cardiomyopathy as reported earlier,<sup>39</sup> we compared EF and FS in Cre vs. non-Cre WT controls. EF and FS of male and female alpha-MHC-MerCreMer mice were comparable with non-Cre WT controls (see [Supplementary material online, Figure S2L and M](#)). These data indicate reduced cardiac function in p62icKO mice is not secondary to the presence of the alpha-MHC-MerCreMer transgene. Importantly, Nbr1 protein expression was not different among groups (see [Supplementary material online, Figure S2N and O](#)). These findings reveal that under normoxic conditions, males are more susceptible than females to inducible depletion of cardiomyocyte p62.

Since myocardial ischaemia precipitates cardiomyocyte hypoxia,<sup>40,41</sup> and because p62 is up-regulated in the context of stress (proteotoxicity, oxidative stress, and apoptosis),<sup>10,42,43</sup> we hypothesized that hypoxia-evoked cardiac stress is exacerbated in p62icKO mice vs. WT littermates. First, it was requisite to determine a duration of hypoxia sufficient to heighten Hif-1 $\alpha$  target genes. Male and female WT mice were exposed to hypoxia for 0.5–6 h,<sup>44</sup> and results were compared with duration-matched male and female WT mice that remained in their cages outside the chamber under normoxic conditions. Six-hour hypoxia elevated mRNA expression of Hif-1 $\alpha$  target genes (*Bnip3* and *Hmox1*) with no mortality (see [Supplementary material online, Figure 3A](#)).

Based on findings from our time-course study, we assessed cardiac function in WT and p62icKO mice exposed to normoxia or 6-h hypoxia. Our hypoxia protocol although reduced EF and FS in WT mice, this reduction did not reach statistical significance ([Figure 1A–C](#); [Supplementary material online, Figure S2J and K](#)). In female p62icKO mice, hypoxia decreased systolic function to a greater degree when compared with p62icKO under normoxia or with WT mice under hypoxia ([Figure 1A–C](#); [Supplementary material online, Figure S2J and K](#)). In male mice, however, p62 deletion already caused a contractile dysfunction (shown by reduced EF and FS) under normoxia, but hypoxia did not exacerbate this contractile defect ([Figure 1A–C](#); [Supplementary material online, Figure S2J and K](#)). These findings indicate female mice are more susceptible to hypoxia-induced contractile dysfunction upon cardiomyocyte selective p62 depletion whereas

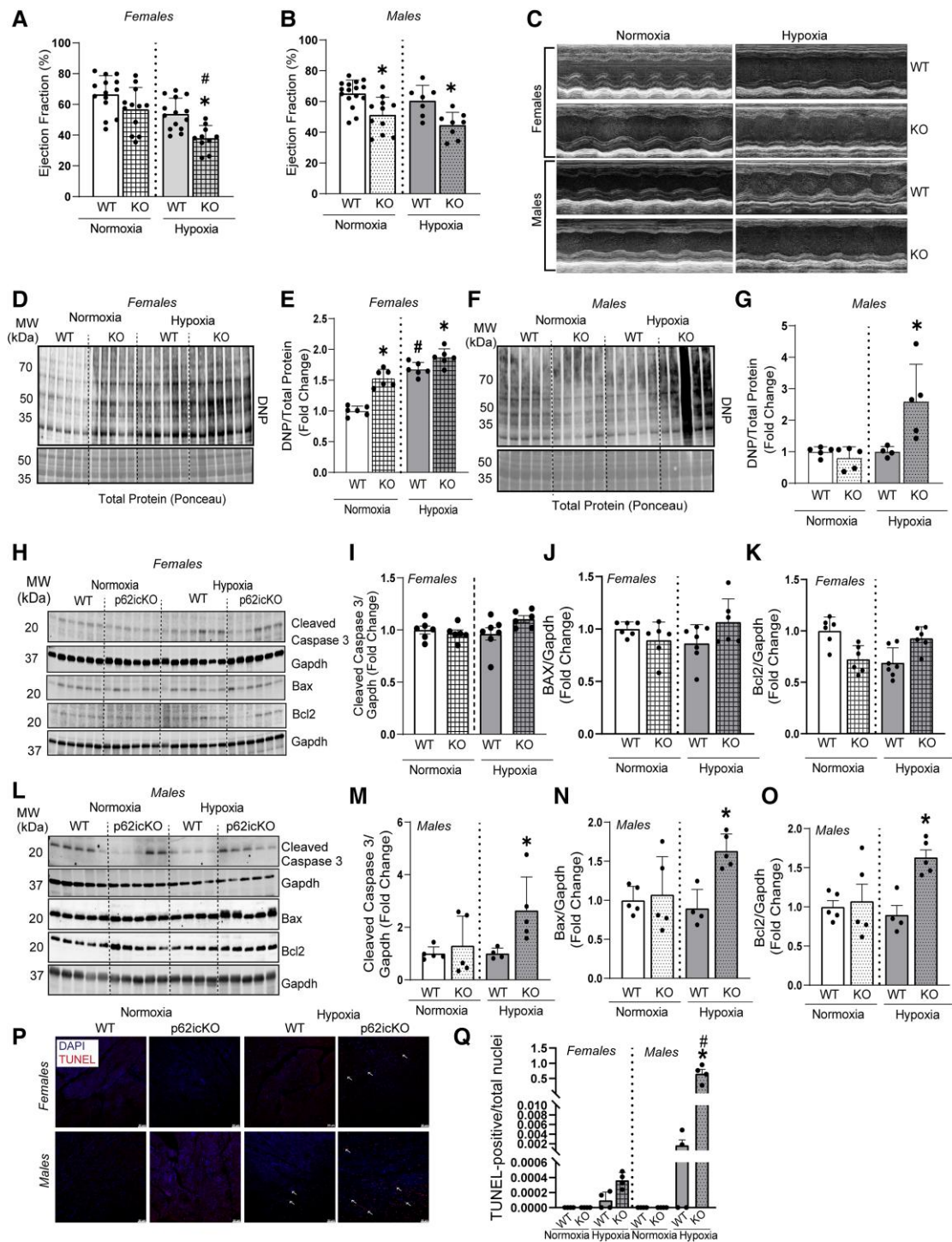


**Figure 1** Mice with acute deletion of p62 (p62icKO) are susceptible to hypoxia. EF expressed as % in (A) female and (B) male p62icKO or WT mice exposed to normoxia or hypoxia measured by echocardiography [ $n = 14$  WT (normoxia) and  $n = 12$  KO (normoxia),  $n = 14$  WT (hypoxia) and  $n = 10$  KO (hypoxia) for female mice (A);  $n = 16$  WT (normoxia) and  $n = 11$  KO (normoxia),  $n = 7$  WT (hypoxia) and  $n = 8$  KO (hypoxia) for male mice] (B). (C) Representative M-mode traces. Representative immunoblots (D, F) and mean densitometry (E, G) for 2,4-dinitrophenylhydrazine (DNP) expression in p62icKO and WT female and male mice exposed to normoxia or hypoxia. Representative immunoblots (H, L) and mean densitometry (I–K and M–O) for cleaved caspase 3, Bax, and Bcl2 to assess apoptosis in female and male mice exposed to normoxia or hypoxia [ $n = 6$ /group WT and KO (normoxia) and  $n = 7$  WT and  $n = 6$  KO (hypoxia) for female mice;  $n = 5$  WT and  $n = 5$  KO (normoxia),  $n = 4$  WT and  $n = 5$  KO (hypoxia) for male mice]. (P) Representative images of TUNEL stained heart sections from males and females WT or p62icKO mice subjected to normoxia or hypoxia ( $n = 4$ /group) and (Q) quantification of the TUNEL images. Data are shown as  $\pm$  standard deviation. Statistical significance between the groups was determined by two-way ANOVA. \* $P < 0.05$ , difference between genotype, i.e. WT and p62icKO groups under the same treatment condition. # $P < 0.05$ , difference between hypoxia and normoxia within the same genotype.

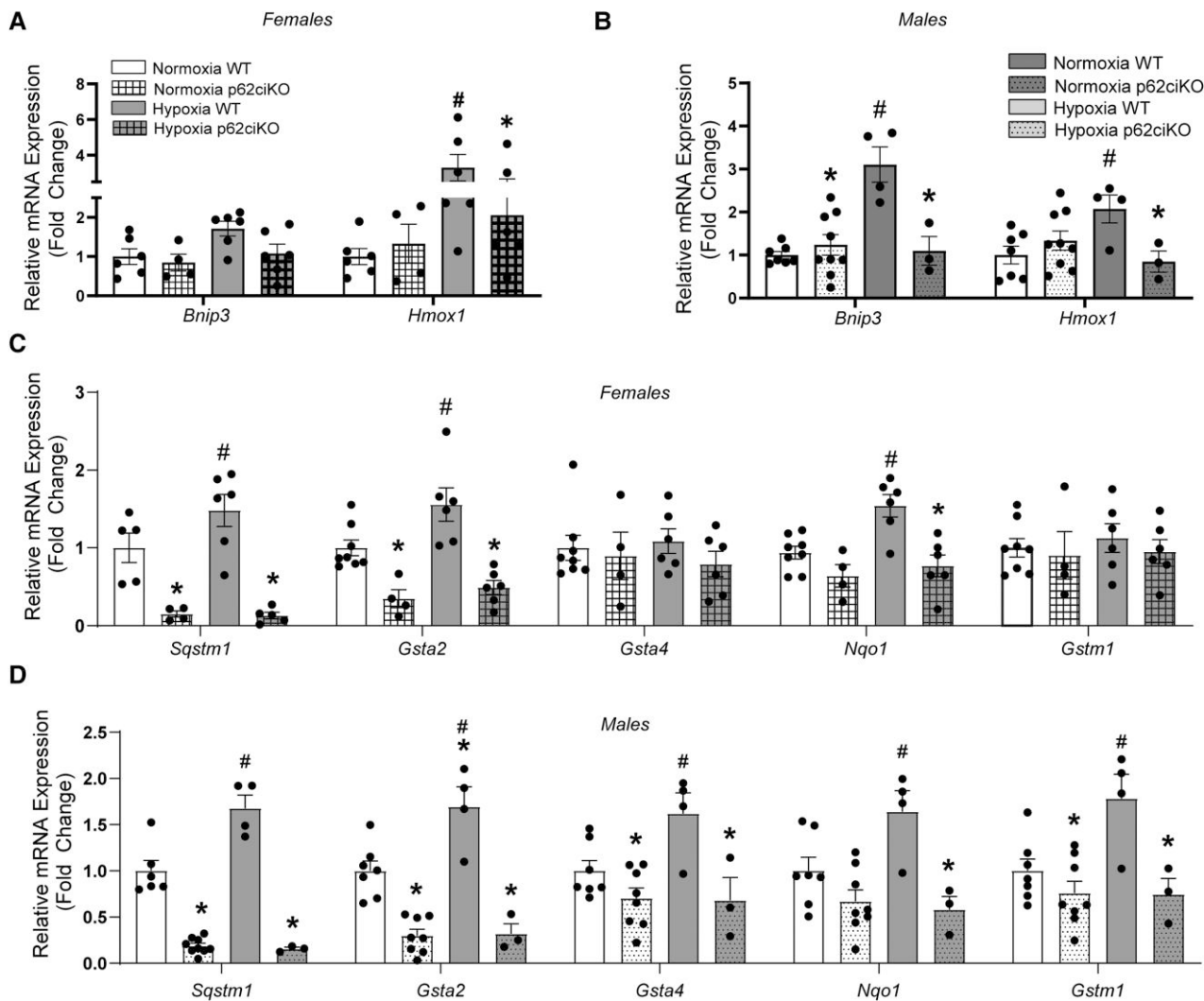


**Figure 2** Cardiomyocyte p62 deletion impairs Hif-1 $\alpha$  and Nrf2 target gene expression under normoxia and hypoxia. mRNA expression of Hif-1 $\alpha$  target genes in hearts from (A) female and (B) male p62icKO or WT mice exposed to normoxia or hypoxia [ $n = 6$  WT and  $n = 4$  KO (normoxia),  $n = 6$  WT and  $n = 6$  KO (hypoxia) for female mice;  $n = 7$  WT and  $n = 9$  KO (normoxia),  $n = 4$  WT and  $n = 3$  KO (hypoxia) for male mice]. mRNA expression of Nrf2 target genes in hearts from (C) female and (D) male p62icKO or WT mice exposed to normoxia or hypoxia [ $n = 5$ – $8$  WT and  $n = 4$  KO (normoxia),  $n = 6$  WT and  $n = 5$ – $6$  KO (hypoxia) for female mice;  $n = 6$ – $7$  WT and  $n = 8$  KO (normoxia),  $n = 4$  WT and  $n = 3$  KO (hypoxia) for male mice]. Data are shown as mean  $\pm$  standard deviation. Statistical significance between the groups was determined by two-way ANOVA. \* $P < 0.05$ , difference between the WT and p62icKO groups within the normoxia or hypoxia group. # $P < 0.05$ , difference between hypoxia and normoxia treatment within the same genotype.

male p62icKO mice already exhibit a decline in contractile function at baseline.

Hypoxia-induced cardiac dysfunction was associated with increased oxidative stress in p62icKO vs. WT mice regardless of sex (Figure 1D–G). Next, to determine the impact of p62 ablation on cell death and apoptosis in male and female hearts exposed to normoxia and hypoxia, we assessed cleaved-caspase 3, B-cell lymphoma 2 (Bcl2), and Bcl-2-associated X-protein (Bax), in addition to performing TUNEL staining. Heightened apoptosis was observed in male (Figure 1L–O) but not in female p62icKO mice subjected to hypoxia (Figure 1H–K). Further, while modest increases in TUNEL-positive nuclei were observed in female p62icKO hypoxic hearts, the response was exacerbated in males (Figure 1P and Q). These results suggest that p62 confers protection from hypoxia to a greater extent in the hearts from male vs. female mice.

### 3.3 Cardiomyocyte p62 deletion impairs Hif-1 $\alpha$ and Nrf2 transcriptional activity

Next, mechanisms responsible for p62-mediated cardioprotection were explored. In cancer cells, p62 regulates hypoxia signalling by stabilizing Hif-1 $\alpha$  via binding with prolyl hydroxylase (PHD) isoform 3 (Phd3), an enzyme important for Hif-1 $\alpha$  degradation.<sup>45</sup> It is unknown whether p62 stabilizes Hif-1 $\alpha$  in the heart to afford protection from hypoxic or ischaemic stress. To test whether p62 modulates responses to cardiac hypoxia, mRNA expression of hypoxia-inducible genes was examined. We found that *Bnip3*, *Hmox1*, and *Sqstm1* (p62) mRNA are elevated in WT hearts exposed to hypoxia, regardless of sex (Figure 2A–D). Of interest, the failure of hypoxia to elevate *Sqstm1* in p62icKO mice was associated with decreased Hif-1 $\alpha$  target gene expression and attenuated Nrf2 transcriptional activity (Figure 2A–D). For example, while hypoxia up-regulated Nrf2 target genes

in WT hearts [e.g. *Sqstm1*, *Gsta2*, and *Nqo1* in females (Figure 2C) and *Sqstm1*, *Gsta2*, *Nqo1*, and *Gstm1* in males (Figure 2D)], the response was attenuated in p62icKO hearts from both sexes. These results are the first to indicate that p62-deficient hearts are more susceptible to hypoxia-induced contractile dysfunction, oxidative stress, and cell death and that this response is associated with a failure to up-regulate both Hif-1 $\alpha$ - and Nrf2-target genes.

### 3.4 Knockdown of p62 reduces Hif-1 $\alpha$ stabilization in H9c2 rat cardiomyoblasts subjected to hypoxia

Deletion of p62 reduced Hif-1 $\alpha$  transcriptional activity in p62icKO hearts. To determine whether hypoxia-induced p62 accumulation is required for Hif-1 $\alpha$  stabilization, H9c2 cells were transfected with p62 or Ctrl siRNA for 48 h and exposed to 21% (normoxia) or 1% (hypoxia) O<sub>2</sub> for 24 h.<sup>46</sup> Congruent with our *in vivo* results, hypoxia increased Hif-1 $\alpha$  and p62 protein expression in H9c2 cells (Figure 3A–C). Compared with H9c2 cells transfected with Ctrl siRNA and exposed to hypoxia, Hif-1 $\alpha$  protein accumulation was reduced after p62 knockdown (Figure 3B).

We next determined whether p62 deletion hindered hypoxia-induced Hif-1 $\alpha$  transcriptional activation. Hypoxia increased *Vegfa*, *Hmx1*, and *Egln1* mRNA in Ctrl siRNA cells, but the response was attenuated after p62 silencing (Figure 3D). Further, since hypoxia is known to cause cell death, we next determined if loss of p62 induced cytotoxicity. In this regard, lactate dehydrogenase (LDH) release was elevated by hypoxia to a greater degree after p62 knockdown vs. Ctrl cells (Figure 3E). These data indicate that p62 contributes importantly to hypoxia-induced Hif-1 $\alpha$  stabilization and transcriptional activation and protects from hypoxia-induced cardiac cell death in H9c2 rat cardiomyoblasts.

### 3.5 Proteasome inhibition during hypoxia recovers Hif-1 $\alpha$ levels after p62 knockdown in H9c2 rat cardiomyoblasts

Under normoxia, Hif-1 $\alpha$  is degraded by the UPS in cancer cells.<sup>47</sup> We tested whether attenuated Hif-1 $\alpha$  stabilization after p62 siRNA is secondary to increased proteasome degradation. Compared with vehicle, the proteasome inhibitor BZ (50 nM) led to further accumulation of p62 both under normoxia and hypoxia in cells transfected with Ctrl siRNA (Figure 3F and G). These data suggest that hypoxia-induced p62 accumulation might be secondary to proteasomal inhibition. Further, the minimal Hif-1 $\alpha$  accumulation in Ctrl siRNA cells under normoxia was elevated markedly upon BZ treatment (Figure 3F and H). Knockdown of p62 did not nullify the BZ-mediated accumulation of Hif-1 $\alpha$ , which was comparable to the Ctrl siRNA cells (Figure 3F and H). These results indicate that p62 plays a key role in hypoxia-induced Hif-1 $\alpha$  stabilization, by inhibiting proteasomal-mediated Hif-1 $\alpha$  degradation.

To gain further insight into how Hif-1 $\alpha$  is degraded in response to p62 silencing, we assessed additional nodes in the hypoxia signalling pathway, including Phd3, factor inhibiting hypoxia-inducible factor (Fih), the E3 ligase Cullin 2, and Von Hippel-Lindau (Vhl).<sup>48,49</sup> These are known to assist with Hif-1 $\alpha$  hydroxylation, ubiquitination, and finally degradation by the UPS.<sup>49</sup> No differences existed among these endpoints in response to normoxia, regardless of the presence or absence of p62. However, hypoxia-induced Hif-1 $\alpha$  protein expression was blunted by p62 knockdown (see Supplementary material online, Figure S3B–D). Further, while Fih expression was unaltered (Figure 3I and Supplementary material online, Figure S3E), Phd3, Vhl, and Cullin 2 were up-regulated with p62 silencing and hypoxia, indicating enhanced Hif-1 $\alpha$  hydroxylation and ubiquitination, preceding its proteasomal degradation (Figure 3I–M). Furthermore, hypoxia increased apoptosis in the Ctrl siRNA transfected cells, a response that was exacerbated upon p62 knockdown (Figure 3I and M). These *in vitro* data are congruent with findings we observed in male p62icKO hearts (Figure 1L–Q). Collectively, our results indicate that p62 is necessary for maintaining stable levels of Hif-1 $\alpha$ , and in its absence, rapid ubiquitination

and proteasome-mediated degradation of Hif-1 $\alpha$  occurs, which ultimately leads to cell death in a hypoxic environment.

### 3.6 Knockdown of p62 promotes proteasomal degradation of Nrf2 in H9c2 rat cardiomyoblasts

In addition to a reduction in hypoxia-sensitive genes, we observed a decrease in Nrf2 target genes in p62icKO hearts exposed to normoxia and hypoxia (Figure 2C and D). Prior reports indicate that Nrf2 is degraded by the proteasome in cancer cells.<sup>34</sup> Thus, we used a reductionist approach to test if p62 depletion increases proteasome-mediated degradation of Nrf2 in cardiac cells. H9c2 rat cardiomyoblasts transfected with p62 or scrambled siRNAs were treated with the proteasomal inhibitor BZ or vehicle control.<sup>30</sup> In vehicle-treated cardiomyoblasts, p62 depletion decreased Nrf2 protein expression (Figure 4A–C), Nrf2 nuclear translocation (Figure 4D and E), and mRNA expression of Nrf2 target genes including *Gdm*, *Gsr*, *Gsta2*, and *Gstm1* (Figure 4F) vs. cells with intact p62. Compared with vehicle-treated cells transfected with scrambled siRNA, BZ increased p62 protein abundance (Figure 4A and B), Nrf2 expression and nuclear translocation (Figure 4A and C–E), and activation of Nrf2 target genes (Figure 4F). In contrast, Keap1 and polyubiquitinated protein abundance increased with BZ independently of genotype (see Supplementary material online, Figure S4A, B, D, and E). These findings substantiate our observation regarding the decrease in Nrf2 transcriptional activity in p62icKO hearts (Figure 2C and D). Further, our results demonstrate that p62, Nrf2, Keap1, and polyubiquitinated proteins are degraded *via* the UPS and that the absence of p62 causes proteasomal degradation of Nrf2 in cardiac cells independently of its mRNA expression (see Supplementary material online, Figure S4C). Further, cytosolic and nuclear fractionation of H9c2 cells transfected with p62 siRNA revealed a decline in Nrf2 levels in both fractions suggesting that a lack of p62 decreases total Nrf2 levels with lesser translocation of Nrf2 into the nucleus (see Supplementary material online, Figure S5A–C). These findings demonstrate that p62 depletion increases UPS-mediated Nrf2 degradation in cardiac cells.

Another important protein degradation pathway that is operational in the heart is macroautophagy.<sup>21,50</sup> Previous studies implicated p62 in the modulation of autophagy in a model of proteotoxic stress in primary cardiomyocytes.<sup>17</sup> To investigate the role of autophagy in the degradation of Nrf2, H9c2 cells transfected with control or p62 targeted siRNAs were treated with vehicle or with the lysosomal inhibitor *Bafilomycin A1* (see Supplementary material online, Figure S6).<sup>25,51</sup> While basal autophagy was not different between the groups, autophagic flux was attenuated in cells transfected with p62 vs. control siRNA (see Supplementary material online, Figure S6A, C, and D). There was a trend for Nrf2 recovery upon lysosomal inhibition (see Supplementary material online, Figure S6A and E) in p62 knockdown cells, which suggests that the autophagy machinery may contribute to Nrf2 degradation in the absence of p62. Keap1, however, was not altered by *BafA1* treatment, regardless of the presence or absence of p62 (see Supplementary material online, Figure S6A and S6G).

### 3.7 Overexpression of p62 stabilizes Nrf2 levels in H9c2 rat cardiomyoblasts

Since the lack of p62 promoted Nrf2 degradation, we reasoned that the gain of p62 might stabilize Nrf2 levels. H9c2 cells transfected with p62 plasmid showed a >1.5-fold increase in p62 protein abundance and a 100-fold increase in p62 mRNA expression (Figure 4G, H, and I). Indeed, overexpression of p62 stabilized Nrf2 protein (Figure 4G and I) and increased Nqo1 protein abundance (Figure 4G–K), whereas Keap1 levels were unchanged (Figure 4G and J). Heightened Nrf2 transcriptional activity in the context of p62 overexpression was confirmed by increased expression of Nrf2 target genes including *Gsta2*, *Gstm1*, *Nqo1*, and *Gpx3* (Figure 4L). Collectively, we provide strong evidence that p62 stabilizes Nrf2 protein expression and transcriptional activity through a mechanism involving the UPS.

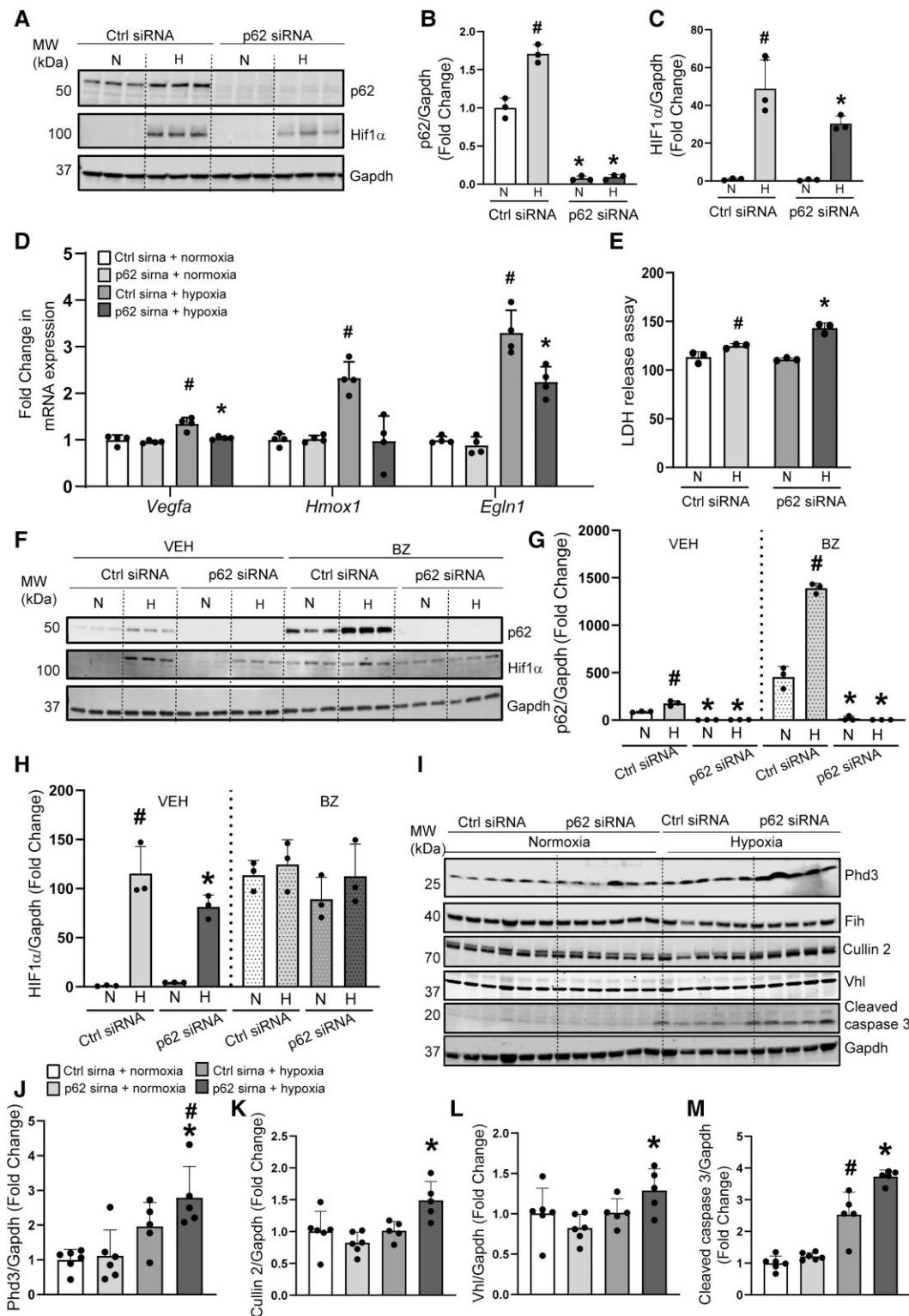


**Figure 3** Knockdown of p62 reduces Hif-1 $\alpha$  stabilization and its transcriptional activity in cultured H9c2 rat cardiomyoblasts exposed to hypoxia. H9c2 cells were transfected with p62 or control (Ctrl) siRNA for 72 h followed by exposure to hypoxia (1% O<sub>2</sub>) or normoxia (21% O<sub>2</sub>) for 24 h. (A) Representative immunoblots (B, C) and mean densitometry of p62 and Hif-1 $\alpha$  normalized to Gapdh. (D) mRNA expression of Hif-1 $\alpha$  target genes. (E) Cytotoxicity measured by LDH release assay. (F) Representative immunoblots and (G, H) mean densitometry of Hif-1 $\alpha$  and p62 in the presence or absence of the proteasome inhibitor BZ. (I) Representative immunoblots for Phd3, Fih, Cullin2, Vhl, and cleaved caspase 3 and (J–M) the corresponding quantification. Quantification for Vhl is provided in [Supplementary material online, Figure S3E](#). Two biological repeats for each group containing three to four samples/group. Data are shown as mean  $\pm$  standard deviation. Statistical significance between the groups was determined by two-way ANOVA. \* $P < 0.05$ , difference between the Ctrl siRNA and p62 siRNA groups within the normoxia (N) or hypoxia (H) group. # $P < 0.05$ , difference between hypoxia and normoxia treatment within the same genotype.



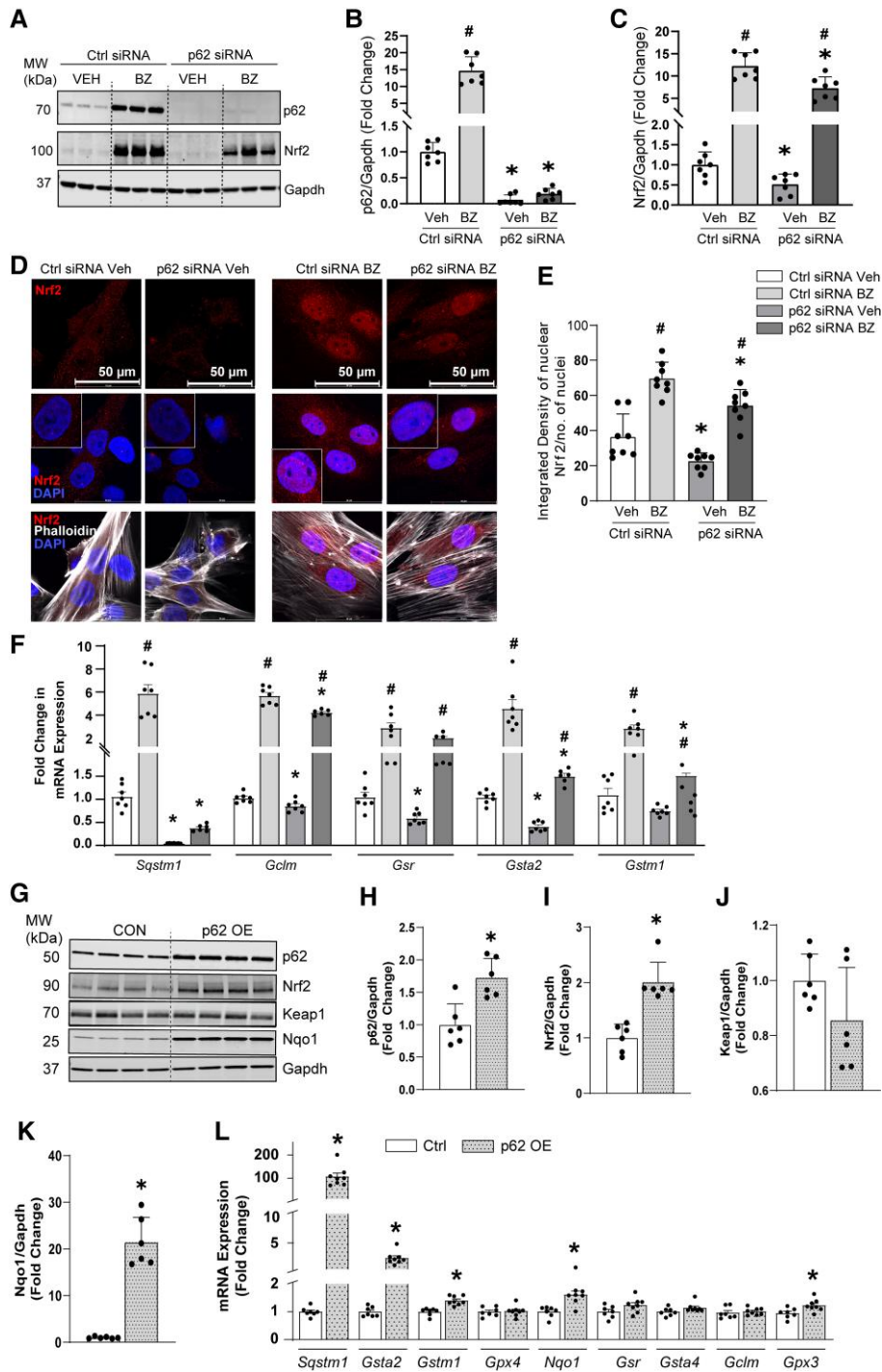


**Figure 4** Loss of p62 decreases and gain of p62 increases Nrf2 protein expression and transcriptional activity in cultured H9c2 cells. H9c2 cells were transfected with p62 or control (Ctrl) siRNA for 72 h and subsequently treated with 25 nM BZ or vehicle (Veh) for 12 h. For gain of p62 studies, H9c2 cells were transfected with a p62 overexpressing (OE) plasmid for 72 h. Control cells were treated similarly but without p62 plasmid transfection. (A) Representative immunoblots and mean densitometry for p62 (B) and Nrf2 (C) normalized to Gapdh. (D) H9c2 cells transfected with Ctrl or p62 siRNA and treated with Veh or BZ were fixed and immunostained for Nrf2 and phalloidin in H9c2 cells. Nuclei were counterstained with DAPI. Images were captured using a confocal microscope at a magnification of  $\times 60$ . Scale bar = 50  $\mu$ m. (E) Nuclear localization of Nrf2 was quantified by measuring the integrated density of staining in the nucleus divided by the total number of nuclei. (F) Several Nrf2 target genes were measured in the cells transfected with Ctrl or p62 siRNA and treated with Veh or BZ. (G) Representative immunoblots and mean densitometry for p62 (H), Nrf2 (I), Keap1 (J), and Nqo1 (K), normalized to Gapdh. (F) mRNA expression of various Nrf2 target genes were determined by qPCR in the control (CON) or p62 OE cells. Two biological repeats for each group containing three to four samples/experiment. Data are shown as mean  $\pm$  standard deviation. For A–F,  $^{\#}P < 0.05$ , difference between the Veh and BZ treated Ctrl siRNA or p62 siRNA groups;  $*P < 0.05$ , difference between the CON and p62 OE groups.  $*P < 0.05$ , difference between the CON and p62 OE groups.

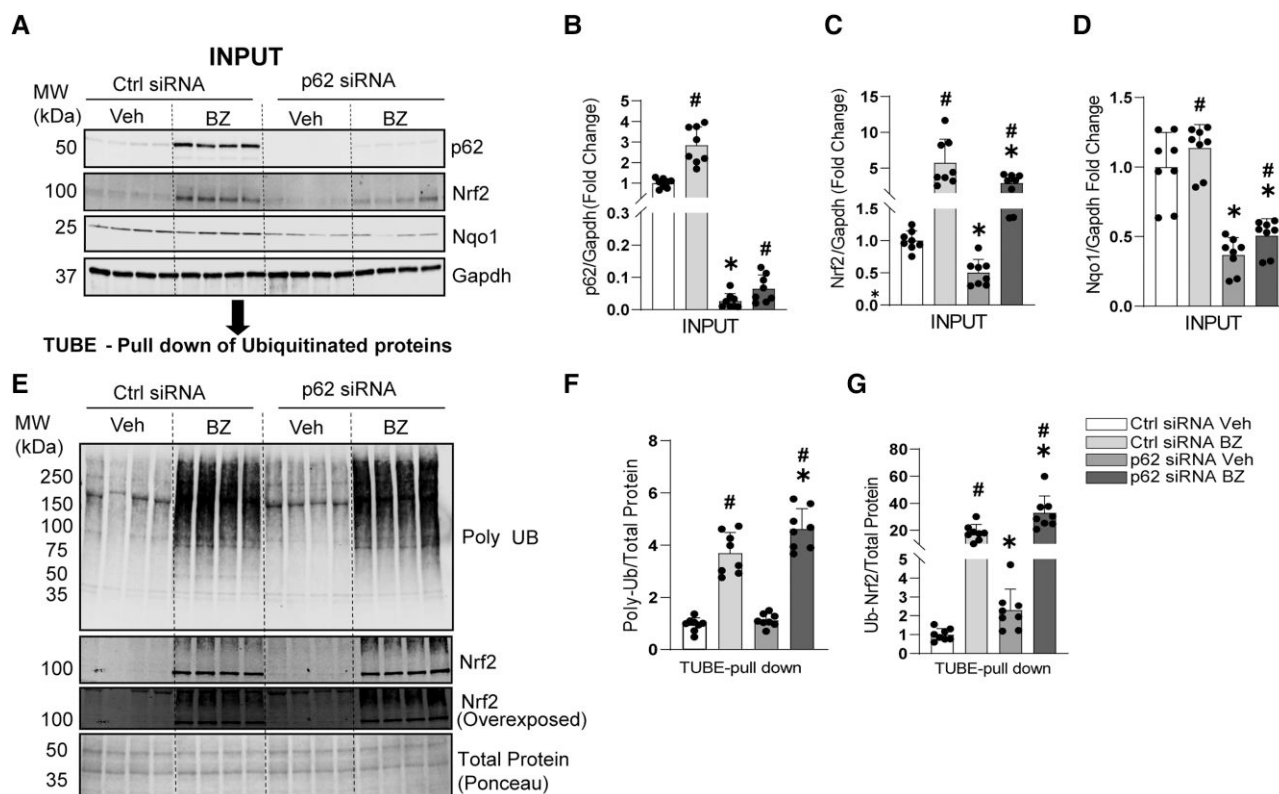


**Figure 5** Loss of p62 induces Nrf2 ubiquitination. H9c2 cells were transfected with p62 or control (Ctrl) siRNA for 72 h and subsequently treated with 25 nM BZ or vehicle (Veh) for 12 h. (A) Representative immunoblots and mean densitometry for p62 (B), Nrf2 (C), and Nqo1 (D), normalized to Gapdh protein. (E) Total cellular ubiquitinated proteins were captured from the INPUT samples using a TUBES assay. Representative immunoblots shows the total poly-ubiquitinated (Ub) and Ub-Nrf2 levels. Because Nrf2 protein is challenging to detect at baseline, we provide an overexposed image of the Ub-Nrf2 blot. The white arrow indicates the baseline Ub-Nrf2 levels. Total protein levels were detected by ponceau staining. Quantifications of poly-Ub (F) and Ub-Nrf2 (G) normalized to total protein levels. Two biological repeats for each group containing four samples/experiment. Data are shown as mean  $\pm$  standard deviation. Two-way ANOVA was utilized to measure the statistical significance between the groups. # $P < 0.05$ , difference between the Veh and BZ treated, Ctrl siRNA or p62 siRNA groups; \* $P < 0.05$ , difference between p62 and Ctrl siRNA transfected cells, treated with Veh or with BZ.

### 3.8 Lack of p62 in H9c2 rat cardiomyoblasts promotes Nrf2-Keap1 co-localization, Nrf2 ubiquitination, and proteasomal degradation

In cancer cells, p62 depletion limits Nrf2 nuclear translocation and subsequent transcriptional activation by promoting Nrf2-Keap1 binding.<sup>52</sup> We tested this possibility in the context of our experimental conditions. In H9c2 cells, we find that a lack of p62 increases Nrf2-Keap1 co-localization regardless of BZ treatment (see [Supplementary material online, Figure S7A and B](#)). These results suggest that p62 is necessary for Nrf2-Keap1 co-localization and Nrf2 stabilization.

A major requirement for proteasomal degradation is the ubiquitination of the targeted substrate.<sup>53</sup> Because our data indicate that proteasomal degradation of Nrf2 is heightened when p62 is lacking in heart cells, we hypothesized that Nrf2 ubiquitination likely is elevated in this context. H9c2 cells transfected with Ctrl or p62-targeted siRNA were treated with BZ or vehicle. In vehicle-treated H9c2 cells, successful deletion of p62 was accompanied by reduced Nrf2 and Nqo1 protein expression (Figure 5A–D), relative to results from p62 intact cells. Upon BZ treatment, H9c2 cells transfected with control siRNA exhibited increased Nrf2 and Nqo1 protein expression that was more robust vs. results from cells transfected with p62 siRNA. In support of our hypothesis, reduced Nrf2 accumulation (i.e. greater degradation) in BZ-treated cells with depleted p62 was associated

with heightened accrual of ubiquitinated proteins (Figure 5E and F) and Nrf2 protein (Figure 5E and G).

Using an alternative approach, we measured Nrf2 degradation in the absence and presence of the protein synthesis inhibitor cycloheximide. In support of our hypothesis and substantiating our earlier findings, the degradation rate of Nrf2 was greater in H9c2 cells transfected with p62 vs. control siRNA (see [Supplementary material online, Figure S8A and B](#)). Collectively, the lack of p62 in cardiac cells increases Nrf2 ubiquitination (Figure 5E and G) and degradation rate *via* the proteasome.

### 3.9 Nrf2 degradation in p62-depleted cells involves Cullin 3

E3 ligases are responsible for ubiquitination of substrate proteins in preparation for proteasomal degradation. The N-terminal region of the E3 ligase Cullin 3 (Cul3) interacts with the intervening region of Keap1 in monkey kidney fibroblast-like cells and human embryonic kidney 293 cells.<sup>54</sup> This Keap1–Cul3 interaction, together with the simultaneous binding of Keap1 to Nrf2, enables Nrf2 ubiquitination and proteasomal degradation. We determined if Cul3 is required for Nrf2 ubiquitination and proteasomal degradation in p62-deficient H9c2 rat cardiomyoblasts. Silencing Cul3 decreased p62 levels in H9c2 cells, whereas p62 depletion did not influence Cul3 (Figure 6A–C). Moreover, the knockdown of Cul3

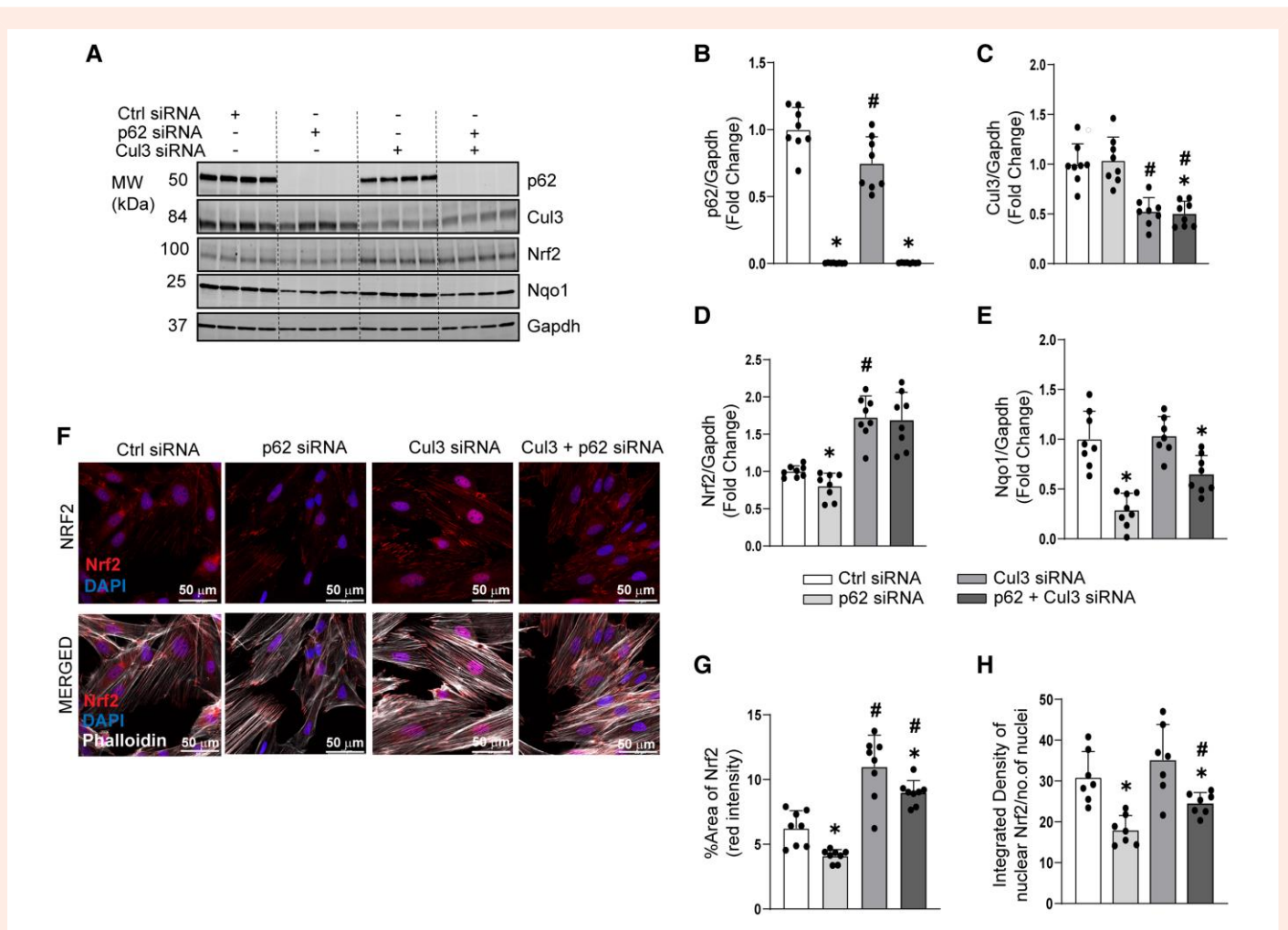


**Figure 6** Nrf2 ubiquitination is mediated by Cullin 3 in H9c2 cells lacking p62. H9c2 cells were transfected with p62 or Cullin 3 (Cul3) targeted siRNA or scrambled (Ctrl) siRNA for 72 h. In parallel experiments, cells were co-transfected with p62 + Cul3 siRNA. (A) Representative immunoblots and mean densitometry for p62 (B), Cul3 (C), Nrf2 (D), and Nqo1 (E) normalized to Gapdh protein. (F) H9c2 cells were immunostained for Nrf2 and phalloidin. Nuclei were counterstained with DAPI. Images were captured using a confocal imager at a magnification of  $\times 60$ . Scale bar = 50  $\mu\text{m}$ . (G) Nrf2 levels was quantified by determining the per cent of staining over the total number of nuclei. (H) Nuclear localization of Nrf2 was quantified by measuring the integrated density of staining in the nucleus over the total number of nuclei. Two biological repeats for each group containing four samples/experiment. Data are shown as mean  $\pm$  standard deviation. Two-way ANOVA was utilized to measure the statistical significance between the groups. \* $P < 0.05$ , difference between the Ctrl siRNA and p62 siRNA or Cul3 siRNA or p62 + Cul3 siRNA groups. # $P < 0.05$ , difference between p62 siRNA and Cul3 siRNA or p62 + Cul3 siRNA groups.

led to Nrf2 accumulation in the presence or absence of p62 (Figure 6A–D). While silencing p62 decreased Nqo1 protein expression, deleting Cul3 partially recovered Nqo1, suggesting that the lack of p62 attenuated Nrf2 nuclear translocation and expression of Nqo1 (Figure 6A and E). Immunostaining revealed an accumulation of cytosolic Nrf2 and a decrease in nuclear Nrf2 levels in cardiomyoblasts co-transfected with Cul3 and p62-targeted siRNA vs. cardiomyoblasts transfected with scrambled or Cul3-targeted siRNA (Figure 6F–H). Taken together, these results indicate Nrf2 ubiquitination is mediated by Cul3 ligase in H9c2 cells.

### 3.10 Loss of p62 decreases cell viability and exacerbates oxidative stress in H9c2 cells

If p62 deficiency reduces Nrf2 translocation to the extent that transcriptional activation of antioxidant genes is compromised, consequences of oxidant stress should be more severe, and we tested this. Glutathione protects cells from oxidative damage by maintaining redox homeostasis.<sup>55</sup>

Nrf2 regulates glutathione homeostasis by regulating glutathione reductase in response to oxidative stress.<sup>56</sup> Since p62 knockdown reduces Nrf2 transcriptional activity, we reasoned that cellular glutathione would be compromised to an extent that heightens oxidative stress. Indeed, total glutathione decreased in response to p62 depletion (see [Supplementary material online, Figure S9A](#)). Buthionine sulfoximine (BSO) is an inhibitor of gamma-glutamylcysteine synthetase that reduces cellular glutathione.<sup>57</sup> Of note, BSO evoked a similar decline in cellular glutathione regardless of intact p62 (see [Supplementary material online, Figure S9A](#)). In a complementary approach, H9c2 cells transfected with control or p62-targeted siRNA were treated with  $\text{H}_2\text{O}_2$ , to induce an extra-cellular oxidant stress. As would be expected based on our findings to this point,  $\text{H}_2\text{O}_2$ -induced cell death (see [Supplementary material online, Figure S9B](#)), accrual of oxidized/carbonylated proteins (see [Supplementary material online, Figure S9C and D](#)), and generation of reactive  $\text{O}_2$  species (see [Supplementary material online, Figure S9E and F](#)) were more robust in H9c2 cells transfected with p62 vs. Ctrl siRNA.

### 3.11 Loss of p62 decreases Nrf2 nuclear translocation in the presence of hypoxia in H9c2 cells

Loss of p62 reduced Hif-1 $\alpha$  and Nrf2 transcriptional activity in p62cKO hearts (Figure 2) and decreased their stabilization in H9c2 cells (Figures 3 and 4A–F). Further, the inability to up-regulate hypoxia-sensitive genes in the context of p62 depletion might be secondary to the lack of Nrf2. Indeed, prior work has shown that these two signalling pathways interact and regulate each other.<sup>30–33</sup> Therefore, we next sought to determine the effect of loss of p62 on Nrf2 protein levels and its nuclear translocation in the absence or presence of hypoxia in H9c2 cells. The *in vitro* results corroborated the *in vivo* evidence that p62 protein accumulation occurs in the Ctrl siRNA cells subjected to hypoxia vs. normoxia (Figure 7A and B). Total Nrf2 protein and its nuclear translocation in response to hypoxia were blunted with p62 knockdown (Figure 7A–D). These results show for the first time that p62 expression and Nrf2 nuclear translocation are enhanced by hypoxia in cardiac cells and thus a possible crosstalk among p62-Nrf2-Hif-1 $\alpha$  exists and requires further investigation.

## 4. Discussion

We tested the hypothesis that loss of cardiomyocyte p62 renders murine hearts more susceptible to hypoxic stress, a characteristic feature of human IHD. Our rationale was based on earlier reports that (i) p62 protects cardiomyocytes from proteotoxic and cytotoxic stress resulting from overexpression of the mutant desmin or CryAB<sup>R120G17</sup> and (ii) diastolic dysfunction evoked by UPS inhibition is exaggerated in mice with whole-body depletion of p62.<sup>18</sup> Since p62 knockdown in CryAB<sup>R120G</sup>-expressing cultured neonatal rat cardiomyocytes evoked a severe phenotype (e.g. cell death and cytotoxicity), and because global p62 deficiency is accompanied by late-onset obesity and insulin resistance, we sought to determine if p62 maintains myocardial function in the context of pathophysiological stress (e.g. hypoxia) using newly generated mice with conditional deletion of p62 in cardiomyocytes.

Our results support a protective role for p62 in hearts exposed to hypoxia. Mechanistically, we revealed that p62 is required for both Hif-1 $\alpha$  and Nrf2 stabilizations in the heart during hypoxia. Thus, when cardiac p62 is lacking, both Hif-1 $\alpha$  and Nrf2 stabilizations are compromised through their proteasomal degradation. The blunted hypoxia-induced Hif-1 $\alpha$  and Nrf2 stabilization in p62 deficient hearts caused cardiac dysfunction, oxidative stress, and cell death.

### 4.1 Mild systolic dysfunction and reduced Nrf2 activation in mice with germline cardiomyocyte-specific p62 deletion

Previous studies examining the role of p62 in the heart used whole-body p62 KO mice. However, these mice develop obesity and systemic insulin resistance, two conditions known to directly affect cardiac metabolism, autophagy, and function.<sup>58,59</sup> To circumvent these effects, we generated mice with cardiomyocyte-specific p62 deletion by crossing p62<sup>lox/lox</sup> mice with *alpha-Mhc-Cre* transgenic animals (i.e. p62cKO mice). Despite high expression of p62 in cardiomyocytes, the cardiac phenotype of p62cKO mice presented as mild systolic dysfunction in male mice under basal (i.e. normoxic) conditions. This is not surprising considering previous work demonstrating that p62 is a stress-inducible protein.<sup>17,18,38,60</sup> Another explanation for the mild cardiac phenotype in the germline p62cKO mice is the compensatory increase we observed regarding Nbr1 mRNA and protein expression. Nbr1 and p62 share structural similarities and they both function as cargo adaptors to enable delivery of ubiquitinated substrates to the UPS or lysosome (*via* the autophagy pathway) for degradation.<sup>61–65</sup> While the direct effect of p62 deletion on Nbr1 function in the heart is unknown, it was reported in mouse primary hepatocytes that Nbr1 overexpression up-regulated p62 mRNA and protein expression and promoted its

phosphorylation, both of which are required for Nrf2 activation.<sup>66,67</sup> The same group showed that while p62 ablation suppressed Nrf2 nuclear translocation, overexpressing Nbr1 increased Nrf2 transcriptional activity in hepatocytes isolated from liver-specific conditional p62 knockout mice. At the gene level, *Nbr1* shares proximity with the *Brca1* tumour suppressor gene. The expression of both *Nbr1* and *Brca1* is controlled by a bidirectional promoter that can be activated by various transcriptional factors involved in the redox homeostasis pathway.<sup>68–70</sup> Deletion of Nbr1 in mouse liver reduced p62-mediated Nrf2 activation during oxidative stress suggesting that both p62 and Nbr1 contribute importantly to Nrf2 regulation.<sup>67</sup> A recent study using a near-haploid human cell line (i.e. HAP1) reported that while p62 is central to the formation of ubiquitin condensate, Nbr1 assists with this process by providing the p62-Nbr1 heterooligomeric complex with a high-affinity UBA domain for selective autophagy of the ubiquitin condensates.<sup>71</sup> In our study, heightened Nbr1 expression might have compensated for reduced cardiomyocyte p62, to thereby minimize the effect of p62 deletion on Nrf2 activation, oxidative stress, and cardiac dysfunction. In carcinoma cells, p62 was down-regulated in response to hypoxia due to enhanced autophagy, and its levels were restored in response to reoxygenation.<sup>72</sup> In the heart, global p62 deletion in the context of ischaemia–reperfusion injury increased infarct size that was associated with elevated LDH release and cell death.<sup>73</sup> To our knowledge, we are the first to show the functional significance of cardiac-specific p62 in response to hypoxia. Experiments investigating whether Nbr1 is required for cardiac Nrf2 activation and preserving responses to hypoxia in the absence and presence of cardiomyocyte p62 are ongoing.

We leveraged unbiased transcriptomics to reveal pathways regulated by p62 that might be responsible for cardiac protection. The inability of p62 repression to significantly influence transcription was not surprising to us because p62 predominately functions as an adaptor protein which co-aggregates with ubiquitinated substrates to facilitate their degradation, thus influencing protein abundance rather than transcript expression.<sup>74</sup> However, our study revealed a selective reduction in Nrf2 target genes, which was further confirmed by qPCR. This result is consistent with the previously established link between p62 and Nrf2-Keap1 pathway in non-cardiac cells.<sup>11,75,76–81</sup>

### 4.2 Sex-specific responses to hypoxia in mice with inducible cardiomyocyte-specific p62 deletion

As opposed to germline p62cKO mice, cardiac-specific inducible p62cKO mice displayed no compensatory increase in Nbr1 protein expression making it a suitable model to study the role of p62 in the heart. Hypoxia (a hallmark feature of IHD) was used to stress hearts from male and female p62cKO mice.<sup>82</sup> In the p62cKO female mice, hypoxia decreased systolic function to a greater degree as compared to normoxia, an effect that was not observed in the male mice (Figure 1A and B).

Because of impaired Hif1 $\alpha$  and Nrf2 signalling, hearts from male p62cKO mice exhibit pronounced oxidative stress, apoptosis, and cell death during hypoxia compared with female KO mice. While sex-specific responses to cardiac stress are a clinically relevant issue, relatively little is known with specific regard to hypoxia. In one report, hypoxia-activated mitogen-activated protein kinase and Jun kinase pathways, secondary to phosphorylation of extra-cellular signal-regulated kinase (ERK1/2) and Jun kinase isotypes, to a greater extent in cardiac fibroblasts from male vs. female mice.<sup>83</sup> A second study reported that intermittent hypoxia decreased glucose tolerance in female mice, the response was amplified in ovariectomized females, but impairments in ovariectomized females could be reversed by treatment with estradiol.<sup>84</sup> Since the heart contains oestrogen and androgen receptors, hormonal regulation of cardiac function during hypoxia is possible.<sup>85</sup> Thus, we postulate that androgen and oestrogen might be candidates for the distinct responses observed in the male and female p62-ablated hearts during hypoxia. Future studies will discern the mechanisms responsible for sex-specific effects in the p62cKO model.

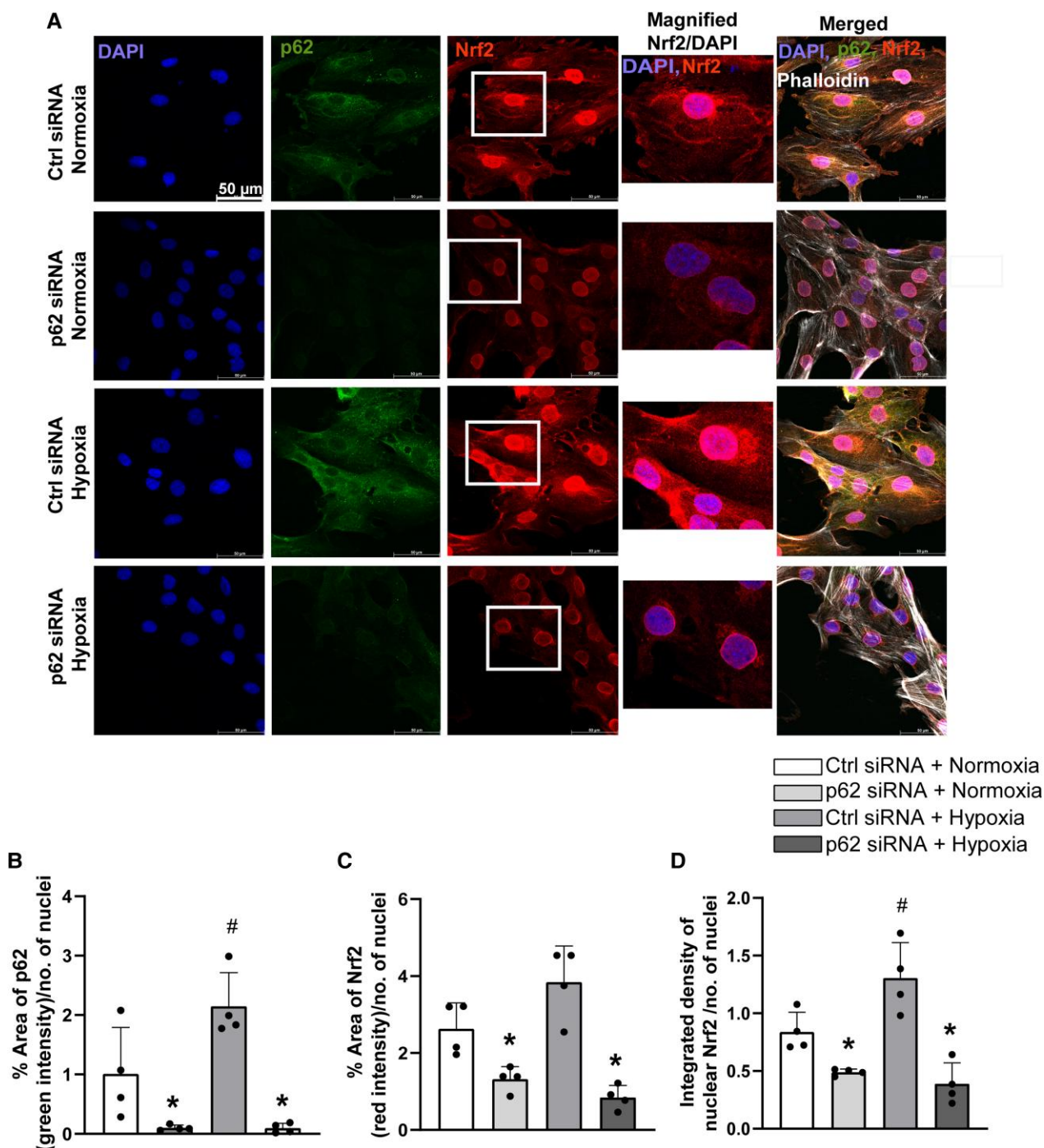


**Figure 7** Hypoxia up-regulates and loss of p62 dampens Nrf2 protein levels. H9c2 cells were transfected with p62 or control (Ctrl) siRNA for 72 h followed by hypoxia (1% O<sub>2</sub>) or normoxia (21% O<sub>2</sub>) treatment for 24 h. (A) The cells were immunostained for p62 (green), Nrf2, and phalloidin. Nuclei were counter-stained with DAPI. Images were captured using a confocal imager at a magnification of ×60. Scale bar = 50 μm. (B–C) p62 and Nrf2 levels were quantified by determining the per cent of staining over the total number of nuclei. (D) Nuclear localization of Nrf2 was quantified by measuring the integrated density of staining in the nucleus over the total number of nuclei. A total of five to eight images were collected/group ( $n = 4$ /group). Mean ± standard deviation is shown. Two-way ANOVA was performed to measure the statistical significance between the groups. \* $P < 0.05$ , difference between the Ctrl and p62 siRNA within the normoxia or hypoxia groups. # $P < 0.05$ , difference between normoxia and hypoxia within Ctrl siRNA or p62 siRNA transfected cells.

### 4.3 Knockdown of p62 induces Cul3-mediated ubiquitination of Nrf2 and its proteasomal degradation in H9c2 rat cardiomyoblasts

We demonstrated that Nrf2 degradation occurs *via* the proteasome, which is preceded by co-localization of Nrf2 with Keap1, followed by Cul-3-mediated Nrf2 ubiquitination. To investigate the role of p62 in this context, experiments were designed based on the non-canonical mechanism by which p62 regulates Nrf2 in hepatocytes.<sup>11</sup> In this regard, Komatsu et al.<sup>11</sup> identified the specific regions where Keap1 (DLG and ETGE motifs) and p62 (KIR motif) interact to enable Nrf2 ubiquitination and degradation. While the latter study focused upon macroautophagy-mediated Keap1 degradation, the influence of p62 on UPS-mediated Nrf2 clearance was not examined. We show that loss of p62 accelerates Nrf2 degradation *via* the proteasome without affecting the level of Keap1. In contrast, Nrf2 stabilization can be achieved by inhibiting the proteasome *via* Cul-3 silencing or by p62 overexpression in H9c2 cardiomyoblasts. When cardiomyoblasts lacking p62 were treated with the proteasomal inhibitor BZ or with Cul-3 siRNA, we were surprised that Nqo1 protein expression did not increase despite Nrf2 accrual. We speculate that this might be secondary to increased Nrf2-Keap1 association coupled with repressed Nrf2 nuclear translocation. We expected heightened Nrf2 degradation, observed in H9c2 cells that lack p62, to associate with increased Keap1 abundance. However, we observed that p62 suppression evoked a decline in Keap1 expression, concurrent with Nrf2 degradation. It is reported that Keap1-independent Nrf2 elimination can occur *via* other E3 ubiquitin ligases.<sup>86–88</sup> Indeed, repression of an E3 ligase (DDB1- and Cullin 4-associated factor 11) up-regulated p62 and stabilized Nrf2 in human neuroglioma cells.<sup>88</sup> Thus, Keap1-independent mechanism(s) may have contributed to Nrf2 ubiquitination and degradation in the context of p62 compromise and ongoing studies are exploring this possibility.

Despite evidence that Keap1 clearance occurs *via* macroautophagy in mouse liver,<sup>89</sup> we did not observe this in H9c2 cells. In contrast, inhibiting UPS catalytic activity led to an accrual of Keap1. Furthermore, we did see a mild reduction in autophagic flux in cells lacking p62, which was associated with a trend for Nrf2 levels to increase ( $P = 0.13$ ). These results suggest that autophagy may modestly contribute to Nrf2 turnover and degradation in cardiac cells.

### 4.4 Cardiomyocyte p62 maintains redox homeostasis and protects from cell death by enabling Hif-1 $\alpha$ and Nrf2 transcriptional activity

To address the concern that compensatory mechanisms might have masked the consequences of germline cardiomyocyte p62 depletion, we examined adult mice with tamoxifen-inducible deletion of p62 (i.e. p62icKO mice). Adult male p62icKO mice exhibited systolic dysfunction in the absence of stress, whereas female p62icKO mice did not display this phenotype at baseline. Importantly, both male and female p62icKO mice developed systolic dysfunction when challenged with hypoxia vs. results from littermate controls, together with heightened oxidative stress and cell death. These findings were accompanied by a decline in Nrf2 target gene expression and provide robust evidence that p62 is required for maintaining redox homeostasis and consequently cardiac protection in response to hypoxic stress. While this study is the first to examine the role of p62 in cardiac responses to hypoxia, Deng et al.<sup>73</sup> showed a robust increase in infarct size in whole-body p62 KO mice subjected to ischaemia/reperfusion, which was associated with increased LDH release and cell death. We further demonstrated that the lack of protection against hypoxia-induced cardiac dysfunction was associated with diminished transcriptional activation of both Hif-1 $\alpha$  and Nrf2 as evidenced by the reduction in the expression of their target genes in p62icKO hearts subjected to hypoxia. Moreover, p62 knockdown in H9c2 cells reduced Hif-1 $\alpha$

stabilization and transcriptional activity during hypoxia. This protective effect of p62 during hypoxia is consistent with the accumulation of p62 under this condition.

In normoxia, PHDs hydroxylate two prolyl residues in Hif-1 $\alpha$  protein rendering it accessible to the Vhl protein, which then targets Hif-1 $\alpha$  for proteasomal degradation.<sup>90–93</sup> Under hypoxia PHDs, activity is reduced and the degradation of Hif-1 $\alpha$  is attenuated, resulting in Hif-1 $\alpha$  stabilization, translocation to the nucleus, and the transcription of hypoxia-responsive genes.<sup>94</sup> Using HeLa cells, Rantanen et al.<sup>45</sup> reported that p62 controls the expression and the localization of Phd3. Specifically, p62 protein levels decreased in response to hypoxia. In contrast, our data indicate p62 accumulates in H9c2 cells exposed to hypoxia. Of interest, we found that several of the important Hif1- $\alpha$  pathway-related proteins Phd3, Cullin 2, and Vhl were up-regulated in the absence of p62 during hypoxia, which presumably contributes to Hif-1 $\alpha$  hydroxylation, ubiquitination, and subsequent proteasomal degradation. While we did not examine Phd3 localization, it is possible that the accumulation of p62 upon hypoxia caused Phd3 aggregation and prevented hydroxylation and proteasomal degradation of Hif-1 $\alpha$ . In this regard, when p62 is depleted, Phd3 becomes less aggregated, which allows it to hydroxylate Hif-1 $\alpha$  and enable its proteasomal degradation. The discrepancy between our study and Rantanen et al.<sup>45</sup> could be due to the cell type employed (HeLa vs. H9c2 cells). Other mechanisms may have contributed to the decrease in Hif-1 $\alpha$  levels in p62 knockdown cells that are PHDs independent. Indeed, Chen et al.<sup>14</sup> demonstrated that p62 regulates Hif-1 $\alpha$  mRNA and protein in cancer cells both under normoxia and in hypoxia through parallel pathways involving the mammalian target of rapamycin, nuclear factor kappa light-chain-enhancer of activated B cell, and the Vhl-Cul-2 complex. One distinction between this study and ours is that (i) we did not observe Hif-1 $\alpha$  changes under normoxia in H9c2 cells and (ii) the effect of p62 on Hif-1 $\alpha$  levels is restricted to hypoxia. This is consistent with our *in vivo* studies and suggests that p62 induction during hypoxia may facilitate Hif-1 $\alpha$  stabilization through a mechanism involving the UPS. Consistent with this idea, Korolchuk et al.<sup>95</sup> demonstrated that p62 accumulation in the presence or absence of autophagy inhibition compromised the degradation of proteins through UPS without affecting its activity in HeLa cells. Thus, we propose that p62 ablation facilitates the delivery of Hif-1 $\alpha$  and Nrf2 to the UPS in cardiac cells. Future studies are required to fully verify this statement.

### 4.5 Summary and conclusions

Results from mice with germline and inducible depletion of cardiomyocyte p62 indicate that this adaptor protein preserves cardiac function, mitigates oxidative stress, and prevents cell death in response to hypoxia. Hearts from these two murine models of cardiomyocyte-specific p62 deletion, together with gain and loss of p62 approaches using H9c2 rat cardiomyoblasts, demonstrate that p62 is required for Hif-1 $\alpha$  and Nrf2 stabilization and transcriptional activity to an extent that maintains redox balance and protects from hypoxic stress. Regarding Nrf2 regulation, lack of p62 heightens Nrf2-Keap1 co-localization, Cul-3-mediated Nrf2 ubiquitination, and Nrf2 proteasomal degradation. These findings substantiate that p62 preserves cardiac redox by stabilizing Nrf2. While the mechanism of how p62 regulates Nrf2 turnover was comprehensively investigated, we acknowledge that p62-mediated Hif-1 $\alpha$  regulation requires additional study. Nevertheless, like Nrf2, Hif-1 $\alpha$  degradation occurs *via* the UPS in cardiac cells. Additionally, we demonstrate for the first time that hypoxia increases Nrf2 transcriptional activity, which is blunted by p62 suppression. Studies investigating the crosstalk among p62-Nrf2-Hif-1 $\alpha$  in the heart are ongoing in our laboratory.

### 4.6 Experimental considerations

Several considerations should be addressed when integrating our findings into what is currently known. First, we did not challenge p62cKO mice with a pathophysiological stressor (e.g. hypoxia). Since p62 is a stress-inducible protein, the mild phenotype displayed by male mice under non-stressed conditions likely would have been exacerbated upon exposure to hypoxia. Second, female p62cKO mice were not examined. Third, the susceptibility

to hypoxia-induced cardiac dysfunction exhibited by female vs. male p62cKO mice was not examined. Whether a sex-specific role for cardiac p62 exists and if an interaction between p62 and estrogen is operational are ongoing topics of investigation in our laboratory. The striking up-regulation of Nbr1 in the context of cardiomyocyte p62 depletion

was unexpected, and at present, we are evaluating the contribution from this protein and other adaptor proteins in the heart that are important for protein degradation. Finally, the interaction between Nrf2 and Hif-1 $\alpha$  in the presence or absence of p62 should be more thoroughly investigated.

## Translational perspective

IHD is a major cause of heart failure and mortality. A characteristic feature of IHD is tissue hypoxia that causes cardiac dysfunction. We demonstrated that intact cardiac p62 exerts protection from hypoxia by stabilizing Hif-1 $\alpha$  and Nrf2.

## Supplementary material

Supplementary material is available at *Cardiovascular Research* online.

## Authors' contributions

R.G. performed the animal and cell experiments, data collection, and figure preparation. A.N.F. and A.J. performed the immunoblots. A.N.F., S.V., and V.V. performed the echocardiography analysis. M.H. and O.M.T.R. helped with the qPCR experiments. O.M.T.R. assisted with the TUNEL assay and A.J. performed the quantifications. M.H. assisted with immunostaining quantification. T.M. assisted with immunohistochemistry and glutathione assay. D.C. and S.S. performed the genotyping of the animals. I.D.C. determined the timeline for hypoxia in p62cKO mice. R.G., S.B., and J.D.S. wrote and edited the manuscript. S.B. conceived the project, acquired the funding, supervised the project, and edited the manuscript. All authors have read and approved the final manuscript.

## Acknowledgements

This work was supported by the National Heart, Lung and Blood Institute (NHLBI) grants R01HL149870-01A1 (S.B.), the National Center for Advancing Translational Sciences (NCATS) grant UL1TR002538 (S.B.), American Heart Association Career Development Award (AHA Award Number: 941327), and RTW Charitable Foundational Grant to R.G. We acknowledge Dr Toru Yanagawa, University of Tsukuba, Japan, for providing the p62 flox mice, Dr Karla M. Pires for establishing the p62cKO and p62cKO mouse lines, and Mrs Diana Lim, a Graphics Specialist in the Molecular Medicine Program at the University of Utah, for her support in preparing the figures presented in this manuscript.

**Conflict of interest:** Authors declare no conflict of interest.

## Data availability

The data underlying this article are available in the article and its online [supplementary material](#). Source data are available from the corresponding authors upon reasonable requests.

## References

1. Tsao CVW, Aday AW, Almarzooq ZI, Alonso A, Beaton AZ, Bittencourt MS, Boehme AK, Buxton AE, Carson AP, Commodore-Mensah Y, Elkind MSV, Evenson KR, Eze-Nliam C, Ferguson JF, Generoso G, Ho JE, Kalani R, Khan SS, Kissela BM, Knutson KL, Levine DA, Lewis TT, Liu J, Loop MS, Ma J, Mussolino ME, Navaneethan SD, Perak AM, Poudel R, Rezk-Hanna M, Roth GA, Schroeder EB, Shah SH, Thacker EL, VanWagner LB, Virani SS, Voecks JH, Wang NY, Yaffe K, Martin SS. Heart disease and stroke statistics—2022 update: a report from the American Heart Association. *Circulation* 2022;**145**:e153–e639.
2. Marzilli M, Merz CN, Boden WE, Bonow RO, Capozza PG, Chillian WM, DeMaria AN, Guarini G, Huqi A, Morrone D, Patel MR, Weintraub WS. Obstructive coronary atherosclerosis and ischemic heart disease: an elusive link!. *J Am Coll Cardiol* 2012;**60**:951–956.
3. Jouett NP, Watenpugh DE, Dunlap ME, Smith ML. Interactive effects of hypoxia, hypercapnia and lung volume on sympathetic nerve activity in humans. *Exp Physiol* 2015;**100**:1018–1029.
4. Waypa GB, Schumacker PT. Hypoxia-induced changes in pulmonary and systemic vascular resistance: where is the O<sub>2</sub> sensor? *Respir Physiol Neurobiol* 2010;**174**:201–211.
5. Giordano FJ. Oxygen, oxidative stress, hypoxia, and heart failure. *J Clin Invest* 2005;**115**:500–508.
6. Jeong SJ, Zhang X, Rodriguez-Velez A, Evans TD, Razani B. P62/SQSTM1 and selective autophagy in cardiometabolic diseases. *Antioxid Redox Signal* 2019;**31**:458–471.
7. Toth RK, Warfel NA. Strange bedfellows: nuclear factor, erythroid 2-like 2 (Nrf2) and hypoxia-inducible factor 1 (HIF-1) in tumor hypoxia. *Antioxidants (Basel)* 2017;**6**:27.
8. Kobayashi M, Yamamoto M. Molecular mechanisms activating the Nrf2-Keap1 pathway of antioxidant gene regulation. *Antioxid Redox Signal* 2005;**7**:385–394.
9. Raghunath A, Sundarraj K, Nagarajan R, Arfuso F, Bian J, Kumar AP, Sethi G, Perumal E. Antioxidant response elements: discovery, classes, regulation and potential applications. *Redox Biol* 2018;**17**:297–314.
10. Nezis IP, Stenmark H. P62 at the interface of autophagy, oxidative stress signaling, and cancer. *Antioxid Redox Signal* 2012;**17**:786–793.
11. Komatsu M, Kurokawa H, Waguri S, Taguchi K, Kobayashi A, Ichimura Y, Sou YS, Ueno I, Sakamoto A, Tong KI, Kim M, Nishito Y, Iemura S, Natsume T, Ueno T, Kominami E, Motohashi H, Tanaka K, Yamamoto M. The selective autophagy substrate p62 activates the stress responsive transcription factor Nrf2 through inactivation of Keap1. *Nat Cell Biol* 2010;**12**:213–223.
12. Lau A, Wang XJ, Zhao F, Villeneuve NF, Wu T, Jiang T, Sun Z, White E, Zhang DD. A non-canonical mechanism of Nrf2 activation by autophagy deficiency: direct interaction between Keap1 and p62. *Mol Cell Biol* 2010;**30**:3275–3285.
13. Jain A, Lamark T, Sjøttem E, Larsen KB, Awuh JA, Overvatn A, McMahon M, Hayes JD, Johansen T. P62/SQSTM1 is a target gene for transcription factor NRF2 and creates a positive feedback loop by inducing antioxidant response element-driven gene transcription. *J Biol Chem* 2010;**285**:22576–22591.
14. Chen K, Zeng J, Xiao H, Huang C, Hu J, Yao W, Yu G, Xiao W, Xu H, Ye Z. Regulation of glucose metabolism by p62/SQSTM1 through HIF1 $\alpha$ . *J Cell Sci* 2016;**129**:817–830.
15. Su H, Wang X. P62 stages an interplay between the ubiquitin–proteasome system and autophagy in the heart of defense against proteotoxic stress. *Trends Cardiovasc Med* 2011;**21**:224–228.
16. Delbridge LMD, Mellor KM, Taylor DJ, Gottlieb RA. Myocardial stress and autophagy: mechanisms and potential therapies. *Nat Rev Cardiol* 2017;**14**:412–425.
17. Zheng Q, Su H, Ranek MJ, Wang X. Autophagy and p62 in cardiac proteinopathy. *Circ Res* 2011;**109**:296–308.
18. Pan B, Li J, Parajuli N, Tian Z, Wu P, Lewno MT, Zou J, Wang W, Bedford L, Mayer RJ, Fang J, Liu J, Cui T, Su H, Wang X. The calcineurin–TFEB–p62 pathway mediates the activation of cardiac macroautophagy by proteasomal malfunction. *Circ Res* 2020;**127**:502–518.
19. Rodriguez A, Duran A, Selloum M, Champy MF, Diez-Guerra FJ, Flores JM, Serrano M, Auwerx J, Diaz-Meco MT, Moscat J. Mature-onset obesity and insulin resistance in mice deficient in the signaling adapter p62. *Cell Metab* 2006;**3**:211–222.
20. Harada H, Warabi E, Matsuki T, Yanagawa T, Okada K, Uwayama J, Ikeda A, Nakaso K, Kirii K, Noguchi N, Bukawa H, Siow RC, Mann GE, Shoda J, Ishii T, Sakurai T. Deficiency of p62/sequestosome 1 causes hyperphagia due to leptin resistance in the brain. *J Neurosci* 2013;**33**:14767–14777.
21. Cho JM, Park SK, Ghosh R, Ly K, Ramos C, Thompson L, Hansen M, Mattered M, Pires KM, Ferhat M, Mookherjee S, Whitehead KJ, Carter K, Buffolo M, Boudina S, Symons JD. Late-in-life treadmill training rejuvenates autophagy, protein aggregate clearance, and function in mouse hearts. *Aging Cell* 2021;**20**:e13467.
22. Pires KM, Torres NS, Buffolo M, Gunville R, Schaaf C, Davis K, Selzman CH, Gottlieb RA, Boudina S. Suppression of cardiac autophagy by hyperinsulinemia in insulin receptor-deficient hearts is mediated by insulin-like growth factor receptor signaling. *Antioxid Redox Signal* 2019;**31**:444–457.

23. Zhang R, Hausladen A, Qian Z, Liao X, Premont RT, Stamler JS. Hypoxic vasodilatory defect and pulmonary hypertension in mice lacking hemoglobin beta-cysteine93 S-nitrosylation. *JCI Insight* 2022;**7**:e155234.
24. Niederkorn M, Ishikawa C KMH, Bartram J, Stepanchick E JRB, Bolanos LC AEC-C, Uible E, Choi K, Wunderlich M, Perentesis JP TMC, Filippi MD, Starczynowski DT. The deubiquitinase USP15 modulates cellular redox and is a therapeutic target in acute myeloid leukemia. *Leukemia* 2022;**36**:438–451.
25. Bharath LP, Cho JM, Park SK, Ruan T, Li Y, Mueller R, Bean T, Reese V, Richardson RS, Cai J, Sargyan A, Pires K, Anandh Babu PV, Boudina S, Graham TE, Symons JD. Endothelial cell autophagy maintains shear stress-induced nitric oxide generation via glycolysis-dependent purinergic signaling to endothelial nitric oxide synthase. *Arterioscler Thromb Vasc Biol* 2017;**37**:1646–1656.
26. Ghosh R, Gillaspie JJ, Campbell KS, Symons JD, Boudina S, Pattison JS. Chaperone mediated autophagy protects cardiomyocytes against hypoxic-cell death. *Am J Physiol Cell Physiol* 2022;**323**:C1555–C1575.
27. Ghosh R, Goswami SK, Feitoza L, Hammock B, Gomes AV. Diclofenac induces proteasome and mitochondrial dysfunction in murine cardiomyocytes and hearts. *Int J Cardiol* 2016;**223**:923–935.
28. Ghosh R, Hwang SM, Cui Z, Gilda JE, Gomes AV. Different effects of the nonsteroidal anti-inflammatory drugs meclizemate sodium and naproxen sodium on proteasome activity in cardiac cells. *J Mol Cell Cardiol* 2016;**94**:131–144.
29. Livak KJ, Schmittgen TD. Analysis of relative gene expression data using real-time quantitative PCR and the 2(-Delta Delta C(T)) method. *Methods* 2001;**25**:402–408.
30. Zheng Q, Su H, Tian Z, Wang X. Proteasome malfunction activates macroautophagy in the heart. *Am J Cardiovasc Dis* 2011;**1**:214–226.
31. Lopitz-Otsoa F, Rodriguez-Suarez E, Aillet F, Casado-Vela J, Lang V, Matthies R, Elortza F, Rodriguez MS. Integrative analysis of the ubiquitin proteome isolated using tandem ubiquitin binding entities (TUBES). *J Proteomics* 2012;**75**:2998–3014.
32. Gilda JE, Ghosh R, Cheah JX, West TM, Bodine SC, Gomes AV. Western blotting inaccuracies with unverified antibodies: need for a western blotting minimal reporting standard (WBMRS). *PLoS One* 2015;**10**:e0135392.
33. Cho JM, Park SK, Kwon OS, La Salle DT, Cerbie J, Fermoye CC, Morgan D, Nelson A, Bledsoe A, Bharath LP, Tandar M, Kanupali SP, Richardson RS, Anandh Babu PV, Mookherjee S, Kishore BK, Wang F, Yang T, Boudina S, Trinity JD, Symons JD. Activating P2Y1 receptors improves function in arteries with repressed autophagy. *Cardiovasc Res* 2023;**119**:252–267.
34. Moscat J, Diaz-Meco MT. P62 at the crossroads of autophagy, apoptosis, and cancer. *Cell* 2009;**137**:1001–1004.
35. Mirrakhimov MM, Kalko TF. Peripheral chemoreceptors and human adaptation to high altitude. *Biomed Biochim Acta* 1988;**47**:89–91.
36. Lamark T, Kirkin V, Dikic I, Johansen T. NBR1 and p62 as cargo receptors for selective autophagy of ubiquitinated targets. *Cell Cycle* 2009;**8**:1986–1990.
37. Kirkin V, Lamark T, Sou YS, Bjorkoy G, Nunn JL, Bruun JA, Shvets E, McEwan DG, Clausen TH, Wild P, Bilusic I, Theurillat JP, Overvatn A, Ishii T, Elazar Z, Komatsu M, Dikic I, Johansen T. A role for NBR1 in autophagosomal degradation of ubiquitinated substrates. *Mol Cell* 2009;**33**:505–516.
38. Tanji K, Odagiri S, Miki Y, Maruyama A, Nikaido Y, Mimura J, Mori F, Warabi E, Yanagawa T, Ueno S, Itoh K, Wakabayashi K. P62 deficiency enhances alpha-synuclein pathology in mice. *Brain Pathol* 2015;**25**:552–564.
39. Koitabashi N, Bedja D, Zaiman AL, Pinto YM, Zhang M, Gabrielson KL, Takimoto E, Kass DA. Avoidance of transient cardiomyopathy in cardiomyocyte-targeted tamoxifen-induced MerCreMer gene deletion models. *Circ Res* 2009;**105**:12–15.
40. Abe H, Semba H, Takeda N. The roles of hypoxia signaling in the pathogenesis of cardiovascular diseases. *J Atheroscler Thromb* 2017;**24**:884–894.
41. Semenza GL. Hypoxia-inducible factor 1 and cardiovascular disease. *Annu Rev Physiol* 2014;**76**:39–56.
42. Nakaso K, Yoshimoto Y, Nakano T, Takeshima T, Fukuhara Y, Yasui K, Araga S, Yanagawa T, Ishii T, Nakashima K. Transcriptional activation of p62/A170/ZIP during the formation of the aggregates: possible mechanisms and the role in Lewy body formation in Parkinson's disease. *Brain Res* 2004;**1012**:42–51.
43. Kuusisto E, Suuronen T, Salminen A. Ubiquitin-binding protein p62 expression is induced during apoptosis and proteasomal inhibition in neuronal cells. *Biochem Biophys Res Commun* 2001;**280**:223–228.
44. Zhang SX, Miller JJ, Gozal D, Wang Y. Whole-body hypoxic preconditioning protects mice against acute hypoxia by improving lung function. *J Appl Physiol (1985)* 2004;**96**:392–397.
45. Rantanen K, Pursiheimo JP, Hogel H, Miikkulainen P, Sundstrom J, Jaakkola PM. P62/SQSTM1 regulates cellular oxygen sensing by attenuating PHD3 activity through aggregate sequestration and enhanced degradation. *J Cell Sci* 2013;**126**:1144–1154.
46. Osuru HP, Lavallee M, Thiele RH. Molecular and cellular response of the myocardium (H9C2 cells) towards hypoxia and HIF-1alpha inhibition. *Front Cardiovasc Med* 2022;**9**:711421.
47. Huang LE, Gu J, Schau M, Bunn HF. Regulation of hypoxia-inducible factor 1alpha is mediated by an O2-dependent degradation domain via the ubiquitin-proteasome pathway. *Proc Natl Acad Sci U S A* 1998;**95**:7987–7992.
48. Luo Z, Tian M, Yang G, Tan Q, Chen Y, Li G, Zhang Q, Li Y, Wan P, Wu J. Hypoxia signaling in human health and diseases: implications and prospects for therapeutics. *Signal Transduct Target Ther* 2022;**7**:218.
49. Schonenberger MJ, Kovacs WJ. Hypoxia signaling pathways: modulators of oxygen-related organelles. *Front Cell Dev Biol* 2015;**3**:42.
50. Ghosh R, Vinod V, Symons JD, Boudina S. Protein and mitochondria quality control mechanisms and cardiac aging. *Cells* 2020;**9**:933.
51. Pattison JS, Osinska H, Robbins J. Atg7 induces basal autophagy and rescues autophagic deficiency in CryABR120G cardiomyocytes. *Circ Res* 2011;**109**:151–160.
52. Ma Q. Role of nrf2 in oxidative stress and toxicity. *Annu Rev Pharmacol Toxicol* 2013;**53**:401–426.
53. Ciechanover A, Schwartz AL. The ubiquitin-proteasome pathway: the complexity and myriad functions of proteins death. *Proc Natl Acad Sci U S A* 1998;**95**:2727–2730.
54. Kobayashi A, Kang MI, Okawa H, Ohtsuiji M, Zenke Y, Chiha T, Igarashi K, Yamamoto M. Oxidative stress sensor Keap1 functions as an adaptor for Cul3-based E3 ligase to regulate proteasomal degradation of Nrf2. *Mol Cell Biol* 2004;**24**:7130–7139.
55. Forman HJ, Zhang H, Rinna A. Glutathione: overview of its protective roles, measurement, and biosynthesis. *Mol Aspects Med* 2009;**30**:1–12.
56. Harvey CJ, Thimmulappa RK, Singh A, Blake DJ, Ling G, Wakabayashi N, Fujii J, Myers A, Biswal S. Nrf2-regulated glutathione recycling independent of biosynthesis is critical for cell survival during oxidative stress. *Free Radic Biol Med* 2009;**46**:443–453.
57. Drew R, Miners JO. The effects of buthionine sulphoximine (BSO) on glutathione depletion and xenobiotic biotransformation. *Biochem Pharmacol* 1984;**33**:2989–2994.
58. Wright JJ, Kim J, Buchanan J, Boudina S, Sena S, Bakirtzi K, Ilkun O, Theobald HA, Cooksey RC, Kandror KV, Abel ED. Mechanisms for increased myocardial fatty acid utilization following short-term high-fat feeding. *Cardiovasc Res* 2009;**82**:351–360.
59. Boudina S, Bugger H, Sena S, O'Neill BT, Zaha VG, Ilkun O, Wright JJ, Mazumder PK, Palfreyman E, Tidwell TJ, Theobald H, Khalimonchuk O, Wayment B, Sheng X, Rodnick KJ, Centini R, Chen D, Litwin SE, Weimer BE, Abel ED. Contribution of impaired myocardial insulin signaling to mitochondrial dysfunction and oxidative stress in the heart. *Circulation* 2009;**119**:1272–1283.
60. Bartlett BJ, Isakson P, Lewerenz J, Sanchez H, Kotzebue RW, Cumming RC, Harris GL, Nezis IP, Schubert DR, Simonsen A, Finley KD. P62, Ref(2)P and ubiquitinated proteins are conserved markers of neuronal aging, aggregate formation and progressive autophagic defects. *Autophagy* 2011;**7**:572–583.
61. Ichimura Y, Kumanomidou T, Sou YS, Mizushima T, Ezaki J, Ueno T, Kominami E, Yamane T, Tanaka K, Komatsu M. Structural basis for sorting mechanism of p62 in selective autophagy. *J Biol Chem* 2008;**283**:22847–22857.
62. Johansen T, Lamark T. Selective autophagy mediated by autophagic adapter proteins. *Autophagy* 2011;**7**:279–296.
63. Liu WJ, Ye L, Huang WF, Guo LJ, Xu ZG, Wu HL, Yang C, Liu HF. P62 links the autophagy pathway and the ubiquitin-proteasome system upon ubiquitinated protein degradation. *Cell Mol Biol Lett* 2016;**21**:29.
64. Danieli A, Martens S. p62-mediated phase separation at the intersection of the ubiquitin-proteasome system and autophagy. *J Cell Sci* 2018;**131**:jcs214304.
65. Rasmussen NL, Kournoutis A, Lamark T, Johansen T. NBR1: the archetypal selective autophagy receptor. *J Cell Biol* 2022;**221**:e202208092.
66. Ichimura Y, Waguri S, Sou YS, Kageyama S, Hasegawa J, Ishimura R, Saito T, Yang Y, Kouno T, Fukutomi T, Hoshii T, Hirao A, Takagi K, Mizushima T, Motohashi H, Lee MS, Yoshimori T, Tanaka K, Yamamoto M, Komatsu M. Phosphorylation of p62 activates the Keap1-Nrf2 pathway during selective autophagy. *Mol Cell* 2013;**51**:618–631.
67. Sanchez-Martin P, Sou YS, Kageyama S, Koike M, Waguri S, Komatsu M. NBR1-mediated p62-liquid droplets enhance the Keap1-Nrf2 system. *EMBO Rep* 2020;**21**:e48902.
68. Whitehouse C, Chambers J, Cateau A, Solomon E. Brca1 expression is regulated by a bidirectional promoter that is shared by the Nbr1 gene in mouse. *Gene* 2004;**326**:87–96.
69. Lee B, Cao R, Choi YS, Cho HY, Rhee AD, Hah CK, Hoyt KR, Obrietan K. The CREB/CRE transcriptional pathway: protection against oxidative stress-mediated neuronal cell death. *J Neurochem* 2009;**108**:1251–1265.
70. Thon M, Al Abdallah Q, Hortschansky P, Scharf DH, Eisendle M, Haas H, Brakhage AA. The CCAAT-binding complex coordinates the oxidative stress response in eukaryotes. *Nucleic Acids Res* 2010;**38**:1098–1113.
71. Turco E, Savova A, Gere F, Ferreri L, Romanov J, Schuschnig M, Martens S. Reconstitution defines the roles of p62, NBR1 and TAX1BP1 in ubiquitin condensate formation and autophagy initiation. *Nat Commun* 2021;**12**:5212.
72. Pursiheimo JP, Rantanen K, Heikinen PT, Johansen T, Jaakkola PM. Hypoxia-activated autophagy accelerates degradation of SQSTM1/p62. *Oncogene* 2009;**28**:334–344.
73. Deng S, Essandoh K, Wang X, Li Y, Huang W, Chen J, Peng J, Jiang DS, Mu X, Wang C, Peng T, Guan JL, Wang Y, Jegga A, Huang K, Fan GC. Tsg101 positively regulates P62-Keap1-Nrf2 pathway to protect hearts against oxidative damage. *Redox Biol* 2020;**32**:101453.
74. Lamark T, Svenning S, Johansen T. Regulation of selective autophagy: the p62/SQSTM1 paradigm. *Essays Biochem* 2017;**61**:609–624.
75. Hayashi K, Dan K, Goto F, Tshuchihashi N, Nomura Y, Fujioka M, Kanzaki S, Ogawa K. The autophagy pathway maintained signaling crosstalk with the Keap1-Nrf2 system through p62 in auditory cells under oxidative stress. *Cell Signal* 2015;**27**:382–393.
76. Yin S, Cao W. Toll-like receptor signaling induces Nrf2 pathway activation through p62-triggered keap1 degradation. *Mol Cell Biol* 2015;**35**:2673–2683.
77. Wang L, Howell MEA, Sparks-Wallace A, Hawkins C, Nickless CA, Kohne C, Hall KH, Moorman JP, Yao ZQ, Ning S. p62-mediated selective autophagy endows virus-transformed cells with insusceptibility to DNA damage under oxidative stress. *PLoS Pathog* 2019;**15**:e1007541.



78. Liao W, Wang Z, Fu Z, Ma H, Jiang M, Xu A, Zhang W. P62/SQSTM1 protects against cisplatin-induced oxidative stress in kidneys by mediating the cross talk between autophagy and the Keap1-Nrf2 signalling pathway. *Free Radic Res* 2019;**53**:800–814.
79. Tang Z, Hu B, Zang F, Wang J, Zhang X, Chen H. Nrf2 drives oxidative stress-induced autophagy in nucleus pulposus cells via a Keap1/Nrf2/p62 feedback loop to protect intervertebral disc from degeneration. *Cell Death Dis* 2019;**10**:510.
80. Wei R, Enaka M, Muragaki Y. Activation of KEAP1/NRF2/P62 signaling alleviates high phosphate-induced calcification of vascular smooth muscle cells by suppressing reactive oxygen species production. *Sci Rep* 2019;**9**:10366.
81. Deng Z, Lim J, Wang Q, Purtell K, Wu S, Palomo GM, Tan H, Manfredi G, Zhao Y, Peng J, Hu B, Chen S, Yue Z. ALS-FTLD-linked mutations of SQSTM1/p62 disrupt selective autophagy and NFE2L2/NRF2 anti-oxidative stress pathway. *Autophagy* 2020;**16**:917–931.
82. Baloglu E. Hypoxic stress-dependent regulation of Na, K-ATPase in ischemic heart disease. *Int J Mol Sci* 2023;**24**:7855.
83. Zhao X, Eghbali-Webb M. Gender-related differences in basal and hypoxia-induced activation of signal transduction pathways controlling cell cycle progression and apoptosis, in cardiac fibroblasts. *Endocrine* 2002;**18**:137–145.
84. Marcouiller F, Jochmans-Lemoine A, Ganouna-Cohen G, Mouchiroud M, Laplante M, Marette A, Bairam A, Joseph V. Metabolic responses to intermittent hypoxia are regulated by sex and estradiol in mice. *Am J Physiol Endocrinol Metab* 2021;**320**:E316–E325.
85. Stumpf WE. Steroid hormones and the cardiovascular system: direct actions of estradiol, progesterone, testosterone, gluco- and mineralcorticoids, and solatriol [vitamin D] on central nervous regulatory and peripheral tissues. *Experientia* 1990;**46**:13–25.
86. Rada P, Rojo AI, Chowdhry S, McMahon M, Hayes JD, Cuadrado A. SCF( $\beta$ )-TrCP promotes glycogen synthase kinase 3-dependent degradation of the Nrf2 transcription factor in a Keap1-independent manner. *Mol Cell Biol* 2011;**31**:1121–1133.
87. Lo JY, Spatola BN, Curran SP. WDR23 regulates NRF2 independently of KEAP1. *PLoS Genet* 2017;**13**:e1006762.
88. Park JY, Kim S, Sohn HY, Koh YH, Jo C. TFEB activates Nrf2 by repressing its E3 ubiquitin ligase DCAF11 and promoting phosphorylation of p62. *Sci Rep* 2019;**9**:14354.
89. Taguchi K, Fujikawa N, Komatsu M, Ishii T, Unno M, Akaike T, Motohashi H, Yamamoto M. Keap1 degradation by autophagy for the maintenance of redox homeostasis. *Proc Natl Acad Sci U S A* 2012;**109**:13561–13566.
90. Cockman ME, Masson N, Mole DR, Jaakkola P, Chang GW, Clifford SC, Maher ER, Pugh CW, Ratcliffe PJ, Maxwell PH. Hypoxia inducible factor- $\alpha$  binding and ubiquitylation by the von Hippel-Lindau tumor suppressor protein. *J Biol Chem* 2000;**275**:25733–25741.
91. Ivan M, Kondo K, Yang H, Kim W, Valiando J, Ohh M, Salic A, Asara JM, Lane WS, Kaelin WG Jr. HIF $\alpha$  targeted for VHL-mediated destruction by proline hydroxylation: implications for O<sub>2</sub> sensing. *Science* 2001;**292**:464–468.
92. Bruick RK, McKnight SL. A conserved family of prolyl-4-hydroxylases that modify HIF. *Science* 2001;**294**:1337–1340.
93. Epstein AC, Gleadle JM, McNeill LA, Hewitson KS, O'Rourke J, Mole DR, Mukherji M, Metzen E, Wilson MI, Dhanda A, Tian YM, Masson N, Hamilton DL, Jaakkola P, Barstead R, Hodgkin J, Maxwell PH, Pugh CW, Schofield CJ, Ratcliffe PJ. C. elegans EGL-9 and mammalian homologs define a family of dioxygenases that regulate HIF by prolyl hydroxylation. *Cell* 2001;**107**:43–54.
94. Kaelin WG. Proline hydroxylation and gene expression. *Annu Rev Biochem* 2005;**74**:115–128.
95. Korolchuk VI, Mansilla A, Menzies FM, Rubinsztein DC. Autophagy inhibition compromises degradation of ubiquitin-proteasome pathway substrates. *Mol Cell* 2009;**33**:517–527.